

A Multiscale Model of Partial Melts 1: Effective Equations

G. Simpson

Department of Mathematics, University of Toronto, Toronto, ON M5S 2E4,
Canada.

M. Spiegelman

Department of Applied Physics and Applied Mathematics, Columbia
University, New York, New York, USA. Lamont-Doherty Earth Observatory,
Palisades, NY 10964, USA.

M. I. Weinstein

Department of Applied Physics and Applied Mathematics, Columbia
University, New York, New York, USA.

G. Simpson, Department of Mathematics, University of Toronto, Toronto, ON M5S 2E4,
Canada. (simpson@math.toronto.edu)

M. Spiegelman, Department of Applied Physics and Applied Mathematics, Columbia Univer-
sity, New York, NY 10027, USA. Lamont-Doherty Earth Observatory, Palisades, NY 10964, USA.
(mspieg@ldeo.columbia.edu)

M. I. Weinstein, Department of Applied Physics and Applied Mathematics, Columbia Univer-
sity, 200 Mudd, New York, NY 10027, USA. (miw2103@columbia.edu)

Abstract. Developing accurate and tractable mathematical models for partially molten systems is critical for understanding the dynamics of magmatic plate boundaries as well as the geochemical evolution of the planet. Because these systems include interacting fluid and solid phases, developing such models can be challenging. The composite material of melt and solid may have emergent properties, such as permeability and compressibility, that are absent in the phase alone. Previous work by several authors have used multiphase flow theory to derive macroscopic equations based on conservation principals and assumptions about interphase forces and interactions. Here we present a complementary approach using homogenization, a multiple scale theory. Our point of departure is a model of the microstructure, assumed to possess an arbitrary, but periodic, microscopic geometry of interpenetrating melt and matrix. At this scale, incompressible Stokes flow is assumed to govern both phases, with appropriate interface conditions.

Homogenization systematically leads to macroscopic equations for the melt and matrix velocities, as well as the bulk parameters, permeability and bulk viscosity, without requiring ad-hoc closures for interphase forces. We show that homogenization can lead to a range of macroscopic models depending on the relative contrast in melt and solid properties such as viscosity or velocity. In particular, we identify a regime that is in good agreement with previous formulations, without including their attendant assumptions. Thus this work serves as independent verification of these models. In addition, homog-

32 enization provides a consistent machinery for computing consistent macro-
33 scopic constitutive relations such as permeability and bulk viscosity that are
34 consistent with a given microstructure. These relations are explored numer-
35 ically in a companion paper.

1. Introduction

Developing quantitative models of partially molten regions in the Earth is critical for understanding the dynamics of magmatic plate boundaries such as mid-ocean ridges and subduction zones, as well as for providing a better integration of geochemistry and geophysics. Beginning in the mid 1980's there have been multiple derivations of macroscopic equations for magma dynamics that describe the flow of a low-viscosity fluid in a viscously deformable, permeable solid matrix [McKenzie, 1984; Scott and Stevenson, 1984, 1986; Fowler, 1985, 1989; Spiegelman, 1993; Stevenson and Scott, 1991; Bercovici et al., 2001a, b; Ricard et al., 2001; Hier-Majumder et al., 2006; Bercovici and Ricard, 2005, 2003; Ricard and Bercovici, 2003; Ricard, 2007]. The details and specific processes included, vary slightly among these model systems but all are derived using the methods of multiphase flow [e.g. Drew and Segel, 1971; Drew, 1971, 1983].

Multiphase flow techniques are well formulated in many texts, including Drew and Passman [1999]; Brennen [2005]. Typically, the two-phase medium is examined at a macroscopic scale, much larger than the pore or grain scale, and one attempts to develop effective media equations based on conservation of mass, momentum, and energy. This approach is reasonably straightforward and has proven useful in applications, notably dilute disperse flows. However, they have two fundamental sources of uncertainty. First, an appropriate “interphase force” must be posited. There is often a tremendous range of mathematically valid choices for this force with little to constrain it beyond physical intuition and experimental validation. Second, the macroscopic equations derived for the partial melt problem include critical constitutive relations, such as permeability, bulk vis-

cosity or effective shear viscosity. These should depend on the microscopic distribution of melt and matrix, information that is often lost in the multiphase flow approach. Multiphase flow does not naturally determine these relationships. As with the interphase force, these closures require estimates from scalings, numerical simulations, and experiments.

In this and a companion paper [Simpson *et al.*, 2008b], we present a complementary method for deriving effective macroscopic equations using the methods of homogenization theory. Rather than assume macroscopic equations and then seek closures for constitutive relations, we assume microscopic equations and derive the macroscopic equations. This is done by a multiple scale expansion, which encodes both fine and coarse length scales into the field variables. As in all multiple scale methods, the equations are matched at each order of the small parameter and solved successively. For a useful introduction to homogenization with applications see Hornung [1997]; Torquato [2002]. More rigorous mathematical treatments are presented in Bensoussan *et al.* [1978]; Sanchez-Palencia [1980]; Cioranescu and Donato [1999]; Chechkin *et al.* [2007]; Pavliotis and Stuart [2008]. Homogenization has been used extensively for flow in rigid and elastic porous media, but we believe this is the first application to the magma dynamics problem which permits viscous deformation of the matrix.

This strategy has several advantages with respect to multiphase flow methods. In particular, there is no under-constrained interphase force, as these effects are described precisely by boundary conditions between the phases at the micro scale. Second, and perhaps more importantly, it provides a mechanism for computing consistent macroscopic constitutive relations for a given microscopic geometry. For the magma dynamics problem, it yields a collection of auxiliary “cell problems” whose solutions determine the bulk viscosity, shear

viscosity, and permeability of the medium consistent with the micro-structure. We emphasize that these macroscopic effective quantities are not volume averages of microscopic quantities. Indeed, permeability and bulk viscosity are undefined at the grain scale, but they appear as macroscopic properties through homogenization. More generally, homogenization can extract tensor valued permeabilities and shear viscosities for anisotropic media. The methods presented are also adaptable to other fine scale rheologies and physics.

In this work, we specifically consider the simplest case of homogenization of the momentum equations for two coupled Stokes problems involving a high viscosity phase (the solid matrix) and a low viscosity fluid. This work is adapted from studies of sintering and partially molten metal alloys, [*Auriault et al.*, 1992; *Geindreau and Auriault*, 1999], which in turn is based on earlier work in poro-elastic media [e.g., *Auriault*, 1987, 1991a; *Auriault and Boutin*, 1992; *Mei and Auriault*, 1989; *Mei et al.*, 1996; *Auriault and Royer*, 2002]. For clarity, we only consider linear viscous behavior for the solid, as this may be appropriate for the diffusion creep regime [e.g., *Hirth and Kohlstedt*, 1995a]. This assumption considerably simplifies the analysis. Extensions to power-law materials are discussed in *Geindreau and Auriault* [1999].

We demonstrate that, depending on the choice of scalings, we can derive homogenized macroscopic equations for three different regimes, and identify a particular regime that is consistent with existing and commonly used formulations such as *McKenzie* [1984] and *Bercovici and Ricard* [2003]. This provides independent validation of these other systems. We also discuss the strengths and weaknesses of homogenization and identifies some open questions. We recognize that the derivation is somewhat technical but have attempted to

make the overall approach as accessible as possible with the hope that other researchers will extend these methods to related problems (e.g., including surface energies and more complex rheologies).

The second paper is more practical and provides specific computation of cell-problems to calculate consistent permeabilities, bulk-viscosities and effective shear viscosities for several simplified pore geometries. In particular we provide a derivation for the bulk viscosity and demonstrate that, for a purely mechanical coupling of phases, it should scale inversely with the porosity; a relationship we conjecture is insensitive to the specifics of the microscopic geometry. Such an inverse relationship has been suggested before [e.g. *Schmeling*, 2000; *Bercovici and Ricard*, 2003]; however, this is the first rigorous derivation from the microscale. Further implications of these results are discussed in the second paper.

Simpson et al. [2008a, b] are based on the PhD. thesis of G. Simpson, *Simpson* [2008].

2. Problem Description

2.1. Macroscopic and Microscopic Domains

To begin the upscaling procedure, we must describe the spatial domains occupied by each phase. We denote with symbol Ω the total macroscopic region of interest, containing both the melt and the matrix, with a characteristic length scale L which might be an observed macroscopic characteristic wavelength (e.g. 1 m–10 km). Initially, we assume that within Ω the matrix has a periodic microstructure. A two-dimensional analog is pictured in Figure 1. Ω , the bounded gray region, is tiled with a fluid filled pore network of period ℓ . ℓ is a representative measure of length scale of the grains or pore distribution,

such as a statistical moment of the grain size distribution, and is much smaller than L .

Notation for the domains is given in Table 1.

We form the first important dimensionless parameter, ϵ ,

$$\epsilon \equiv \frac{\ell}{L} \quad (1)$$

ϵ will play two important roles in what follows. First, all other dimensionless numbers and parameters will be expressed in powers of ϵ . Second, we will expand the dependent variables in powers in ϵ as in

$$\Phi = \Phi^{(0)} + \epsilon\Phi^{(1)} + \epsilon^2\Phi^{(2)} + \dots \quad (2)$$

Of course, real partially molten rocks are not a periodic medium. Pore structures similar to those expected in peridotite appear in Figure 3. Since it is crystalline, there is some regularity, but it is closer to a *random* medium. While only the periodic case is treated in this work, the random one is of interest and is also amenable to homogenization, *Torquato* [2002].

We divide our domain Ω from Figure 1 into three subregions:

Ω_f —The fluid portion of Ω .

Ω_s —The solid portion of Ω .

Γ —The interface between fluid and solid in Ω .

We shall write equations for the melt in Ω_f , equations for the matrix in Ω_s , and boundary conditions between the two along Γ .

We now introduce the notion of a cell. The cell, appearing in Figure 2 and denoted with the symbol Y , is a scaled, dimensionless, copy of the periodic microstructure of Figure 1.

This is divided into a fluid region, Y_f , a solid region, Y_s , and an interface, γ . A simple

three-dimensional example of such a cell appears is displayed in Figure 4. The cell should be interpreted as a scaled representative elementary volume of the grain scale. It may be a single grain or a small ensemble of grains.

Although the connectedness of both phases is an important property, the particular microstructure of Y does not play a significant role in the form of macroscopic equations. Cell geometry does determine the magnitudes and forms of the constitutive relations appearing in the equations. This is discussed in the companion paper.

2.2. Grain Scale Equations

At the microscale, we assume both phases are incompressible, linearly viscous, isotropic fluids. The rheology for each phase is:

$$\sigma = -pI + 2\mu e(\mathbf{v}) \quad (3)$$

where $e(\mathbf{v})$ is the strain-rate tensor,

$$e(\mathbf{v}) = \frac{1}{2} (\nabla \mathbf{v} + (\nabla \mathbf{v})^T) \quad (4)$$

Components may be accessed by index notation:

$$e_{ij}(\mathbf{v}) = \frac{1}{2} \left(\frac{\partial v_i}{\partial X_j} + \frac{\partial v_j}{\partial X_i} \right)$$

$$\sigma_{ij} = -p\delta_{ij} + 2\mu e_{ij}(\mathbf{v})$$

The variable \mathbf{X} appearing in these expressions denotes the dimensional spatial variable. The stress in Ω_s for the solid phase is σ^s , with pressure p^s and velocity \mathbf{v}^s . Similarly, the fluid has stress σ^f , pressure p^f , and velocity \mathbf{v}^f in Ω_f . The notation for the fields is given in Table 2.

At the pore scale, the Reynolds number is small; using the the values of Table 3, the value in the melt is $\lesssim O(10^{-5})$ and as low as $O(10^{-30})$ in the matrix. Therefore, we will

omit inertial terms in the conservation of momentum equations. Each phase satisfies the Stokes equations at the grain scale; the divergence of the stress of each phase balances the body forces. As we are interested in buoyancy driven flow, the forces $\mathbf{g}^s \equiv -\rho_s g \mathbf{e}_3$ and $\mathbf{g}^f \equiv -\rho_f g \mathbf{e}_3$ are included. The equations are:

$$\nabla \cdot \sigma^f + \mathbf{g}^f = 0 \quad \text{in } \Omega_f \qquad \nabla \cdot \sigma^s + \mathbf{g}^s = 0 \quad \text{in } \Omega_s \qquad (5a)$$

$$\nabla \cdot \mathbf{v}^f = 0 \quad \text{in } \Omega_f \qquad \nabla \cdot \mathbf{v}^s = 0 \quad \text{in } \Omega_s \qquad (5b)$$

Conditions at the interface between fluid and solid, Γ , are still needed. As both are viscous, we posit continuity of velocity and normal stress:

$$\mathbf{v}^s = \mathbf{v}^f, \quad \text{on } \Gamma \qquad (6a)$$

$$\sigma^s \cdot \mathbf{n} = \sigma^f \cdot \mathbf{n}, \quad \text{on } \Gamma \qquad (6b)$$

146 A Boussinesq approximation has been made by taking the velocities to be continuous
 147 as opposed to the momenta. These equations are exact in the sense that, subject to
 148 boundary conditions on the exterior of Ω , solving them would provide a full description
 149 of the behavior of the two-phase medium (although it would be impractical to solve such
 150 a system at the macroscopic scale of interest).

2.3. Scalings

Our effective equations emerge from multiple scale expansions of the dependent variables. The dimensional spatial variable \mathbf{X} specifies a position within either Ω_s or Ω_f . We introduce two dimensionless spatial scales, \mathbf{y} , the “fast” spatial scale, and \mathbf{x} , the “slow”

spatial scale. These relate to \mathbf{X} , and one another, as:

$$\mathbf{y} \equiv \mathbf{X}/\ell \quad (7a)$$

$$\mathbf{x} \equiv \mathbf{X}/L = \epsilon \mathbf{y} \quad (7b)$$

The expansion in (2) is now made more precise. All variables are assumed, initially, to have both fast and slow scale dependence:

$$\Phi(\mathbf{y}) = \Phi^{(0)}(\epsilon \mathbf{y}, \mathbf{y}) + \epsilon \Phi^{(1)}(\epsilon \mathbf{y}, \mathbf{y}) + \epsilon^2 \Phi^{(2)}(\epsilon \mathbf{y}, \mathbf{y}) + \dots \quad (8)$$

151 Such an expansion captures grain scale detail in the second argument, while permitting
 152 slow, macroscopic variations in the first argument. As we take our domain to be peri-
 153 odically tiled with scaled copies of the cell Y , we assume $\Phi^{(j)}(\mathbf{x}, \mathbf{y})$ is \mathbf{y} -periodic at all
 154 orders of j . We seek equations that are only functions of \mathbf{x} ; these will be the effective
 155 macroscopic equations.

Before making series expansions in powers of ϵ , the equations must be scaled appropriately. In addition to ϵ , there are several other important dimensionless numbers. As motivation, let P^s , P^f , V^s , V^f be characteristic pressures and velocities for the solid and fluid phases. We write:

$$p^f = P^f \tilde{p}^f \quad p^s = P^s \tilde{p}^s \quad (9)$$

$$\mathbf{v}^f = V^f \tilde{\mathbf{v}}^f \quad \mathbf{v}^s = V^s \tilde{\mathbf{v}}^s \quad (10)$$

Tildes reflect that the variables are now dimensionless and $O(1)$. Using these definitions, we non-dimensionalize (5a). We are free to scale the equations to either the slow or fast length scale. In this work, we scale to the ℓ length, though this does not affect the results.

On the length scale ℓ , the force equations are:

$$\begin{aligned} \nabla_y \cdot \left[-\tilde{p}^f I + \left(\frac{\mu_f V^f}{P^f \ell} \right) 2\tilde{\mu}_f e_y(\tilde{\mathbf{v}}^f) \right] + \frac{\rho_f g \ell}{P^f} \tilde{\mathbf{g}}^f &= 0 \\ \nabla_y \cdot \left[-\tilde{p}^s I + \left(\frac{\mu_s V^s}{P^s \ell} \right) 2\tilde{\mu}_s e_y(\tilde{\mathbf{v}}^s) \right] + \frac{\rho_s g \ell}{P^s} \tilde{\mathbf{g}}^s &= 0 \end{aligned} \quad (11)$$

where e_y denotes the strain-rate tensor with velocity gradients taken with respect to the fast length scale y . This motivates defining four more dimensionless numbers:

$$\mathcal{Q}_\ell^f \equiv \frac{\mu_f V^f}{P^f \ell} \quad \mathcal{Q}_\ell^s \equiv \frac{\mu_s V^s}{P^s \ell} \quad (12)$$

$$\mathcal{R}_\ell^f \equiv \frac{\rho_f g \ell}{P^f} \quad \mathcal{R}_\ell^s \equiv \frac{\rho_s g \ell}{P^s} \quad (13)$$

The \mathcal{Q} 's measure the relative magnitudes of the viscous forces and the pressure gradients, while the \mathcal{R} 's measure the relative magnitudes of the body forces and the pressure gradients. The $\tilde{\mu}$'s and $\tilde{\mathbf{g}}$'s remain in the equations as $O(1)$ constants. Three other important parameters are the ratio of the viscosities of the two phases, the ratio of the velocities of the two phases, and the ratio of the pressures of the phases:

$$\mathcal{M} \equiv \frac{\mu_f}{\mu_s} \quad (14)$$

$$\mathcal{V} \equiv \frac{V^f}{V^s} \quad (15)$$

$$\mathcal{P} \equiv \frac{P^f}{P^s} \quad (16)$$

¹⁵⁶ A full list of dimensionless numbers is given in Table 4.

Starting with ϵ , \mathcal{V} , and \mathcal{M} , we estimate these parameters with the data in Table 3:

$$\mathcal{M} = O(10^{-21} - 10^{-14}) \quad (17)$$

$$\mathcal{V} = O(10^1 - 10^3) \quad (18)$$

$$\epsilon = O(10^{-7} - 10^{-2}) \quad (19)$$

For these values, $\mathcal{M} \ll \epsilon \ll \mathcal{V}$. Since we expand the equations in powers of ϵ , we relate all quantities to ϵ . A quantity Q is said to be $O(\epsilon^p)$ if

$$\epsilon^{p+1} \ll Q \ll \epsilon^{p-1} \quad (20)$$

In terms of ϵ , \mathcal{M} and \mathcal{V} are approximately:

$$\mathcal{M} = O(\epsilon^{11} - \epsilon^2) \quad (21)$$

$$\mathcal{V} = O(\epsilon^0 - \epsilon^{-2}) \quad (22)$$

157 We emphasize that this power of ϵ scale is less precise than a power of 10 scale. For
158 example, \mathcal{V} might be $O(10^1)$, but if $\epsilon = O(10^{-4})$, we would say $\mathcal{V} = O(\epsilon^0 = 1)$ since
159 $\mathcal{V} \ll \epsilon^{-1}$. Indeed, in one of the scaling regimes we consider, $\mathcal{V} = O(\epsilon^0 = 1)$.

To estimate the other parameters, we need estimates of the characteristic pressures. To do this, we first consider the forces on the matrix. At the macroscopic scale, the melt is $O(1\%)$ of the medium's volume. We thus argue that on this scale, the matrix is “close” to satisfying the Stokes equations; the pressure gradient, viscous forces, and gravity balance one another. On the large length scale L , the dimensionless form of (5a) is

$$\nabla_x \cdot \left[-\tilde{p}^s I + \left(\frac{\mu_s V^s}{P^s L} \right) 2\tilde{\mu}_s e_x(\tilde{\mathbf{v}}^s) \right] + \frac{\rho_s g L}{P^s} \tilde{\mathbf{g}}^s = 0. \quad (23)$$

Similar to Equation (11), we define

$$\mathcal{Q}_L^s \equiv \frac{\mu_s V^s}{P^s L} \quad (24)$$

$$\mathcal{R}_L^s \equiv \frac{\rho_s g L}{P^s} \quad (25)$$

For the terms to be in balance, $\mathcal{Q}_L^s = O(1)$ and $\mathcal{R}_L^s = O(1)$. Using (24–25) and the definition of ϵ , the fast length scale parameters are:

$$\mathcal{Q}_\ell^s = O(\epsilon^{-1}) \quad (26)$$

$$\mathcal{R}_\ell^s = O(\epsilon^1) \quad (27)$$

In the absence of direct pressure measurements, we assume the pressures are the same order,

$$\mathcal{P} = O(1 = \epsilon^0). \quad (28)$$

An argument for this is given in *Drew* [1983]. Briefly, since the velocities of interest are far less than the speed of sound, it would be difficult to support large pressure gradients across the phases without surface tension, a mechanism we do not include. We make an additional assumption that there are $O(1)$ non-hydrostatic pressures in both phases; if $p = p_{\text{hydro}} + p_{\text{non-hydro}}$ then

$$\left| \frac{p}{p_{\text{non-hydro}}} \right| = O(1 = \epsilon^0). \quad (29)$$

In the fluid, since $\rho_f/\rho_s = O(1)$, a consequence of $\mathcal{P} = O(1)$ is

$$\mathcal{R}_\ell^f = \frac{\rho_f g \ell}{P^f} = \frac{\rho_s g \ell}{P^s} \frac{\rho_f}{\rho_s} \frac{P^s}{P^f} = \mathcal{R}_\ell^s \frac{\rho_f}{\rho_s} \mathcal{P} = O(\epsilon^1) \quad (30)$$

The fluid's force ratio is

$$\mathcal{Q}_\ell^f = \frac{\mu_f V^f}{P^f \ell} = O(\mathcal{P} \mathcal{M} \mathcal{V} \mathcal{Q}_\ell^s) = O(\epsilon^{-1} \mathcal{M} \mathcal{V}) \quad (31)$$

and

$$\mathcal{Q}_L^f = \mathcal{M} \mathcal{V} \quad (32)$$

Therefore,

$$\mathcal{M}V = O(\epsilon^{10} - \epsilon^1) \quad (33)$$

$$\mathcal{Q}_\ell^f = O(\epsilon^9 - \epsilon^0) \quad (34)$$

The choice of dimensionless parameters will lead to different expansions and effective equations. In the terminology of *Auriault* [1991a, b]; *Geindreau and Auriault* [1999]; *Auriault et al.* [1992], we can derive one of several outcomes: *biphasic* media, *monophasic* media, and *non-homogenizable* media. In the biphasic case, the macroscopic description possesses a distinct velocity field for each phase. In the monophasic case *both* phases have the same velocity field and we have a single, hybrid, material. In both biphasic and monophasic models, there is only one pressure. The non-homogenizable case is explained in Appendix D.

From here on, we assume

$$\boxed{\mathcal{Q}_\ell^f = O\left(\frac{\mathcal{M}\mathcal{V}}{\epsilon}\right) = O(\epsilon)} \quad (35)$$

which implies that at the microscale, the ratio of viscous stresses to pressure in the liquid phase is $O(\epsilon)$. This includes two biphasic cases, $(\mathcal{M}, \mathcal{V}) = (O(\epsilon^2), O(1))$ and $(\mathcal{M}, \mathcal{V}) = (O(\epsilon^3), O(\epsilon^{-1}))$, and a related monophasic case. We discuss the significance of constraint (35) in Section 4.1.

2.4. Main Results

Before proceeding with the expansions, we state our main results. The dependent variables are \mathbf{V}^s , the leading order velocity in the matrix, P , the leading order (fluid) pressure, and \mathbf{V}^f , the leading order mean velocity in the fluid. Full notation is given in Table 5.

The following systems of equations are derived in Section 3 and Appendices A–C by multiple scale expansions. They employ an additional assumption that the cell microstructure possesses certain symmetries which are discussed in Section 3.6 and Appendix E.

Biphasic-I: In the first biphasic case, $\mathcal{V} = O(1)$ and $\mathcal{M} = O(\epsilon^2)$, the leading order non-dimensional equations are:

$$0 = \bar{\rho}\mathbf{g} - \nabla P + \nabla \cdot \left[\left(\zeta_{\text{eff.}} - \frac{2}{3}\mu_s(1 - \phi) \right) \nabla \cdot \mathbf{V}^s \right] \quad (36a)$$

$$+ \nabla \cdot [2(1 - \phi)\mu_s e(\mathbf{V}^s)] + \nabla \cdot [2\eta_{\text{eff.}}^{lm} e_{lm}(\mathbf{V}^s)]$$

$$\phi(\mathbf{V}^f - \mathbf{V}^s) = -\frac{k_{\text{eff.}}}{\mu_f} (\nabla P - \mathbf{g}^f) \quad (36b)$$

$$\nabla \cdot [\phi \mathbf{V}^f + (1 - \phi) \mathbf{V}^s] = 0 \quad (36c)$$

Again, we emphasize that the assumption $\mathcal{V} = O(1 = \epsilon^0)$ does not imply that the melt and solid velocities are equal, simply that the ratio of the viscosities is of significantly different order than the ratio of the velocities. The lm terms are summed over all pairs of l and m . $k_{\text{eff.}}$ is a scalar permeability (and more generally a second order tensor), $\zeta_{\text{eff.}}$ is an effective scalar bulk viscosity, and for each pair of indices (l, m) , $\eta_{\text{eff.}}^{lm}$ is the anisotropic contribution to the effective shear viscosity, a second order tensor. These material properties, defined in terms of microscale “cell problems” have been simplified through the domain symmetries. Derivatives are taken with respect to the dimensionless macroscopic scale \mathbf{x} , which we have suppressed as a subscript for clarity. We note that the equations for the Biphasic-I scaling are in good agreement with previous formulations. The chief difference is the appearance $\eta_{\text{eff.}}$ term capturing the grain scale anisotropy, which is new.

Biphasic-II: In the second biphasic case, $\mathcal{V} = O(\epsilon^{-1})$ and $\mathcal{M} = O(\epsilon^3)$, the macroscopic system is:

$$0 = \bar{\rho}\mathbf{g} - \nabla P + \nabla \left[\left(\zeta_{\text{eff.}} - \frac{2}{3}\mu_s(1 - \phi) \right) \nabla \cdot \mathbf{V}^s \right] \quad (37a)$$

$$+ \nabla \cdot [2(1 - \phi)\mu_s e(\mathbf{V}^s)] + \nabla \cdot [2\eta_{\text{eff.}}^{lm} e_{lm}(\mathbf{V}^s)]$$

$$\phi \mathbf{V}^f = -\frac{k_{\text{eff.}}}{\mu_f} (\nabla P + \mathbf{g}^f) \quad (37b)$$

$$\nabla \cdot (\phi \mathbf{V}^f) = 0 \quad (37c)$$

$\zeta_{\text{eff.}}$, $\eta_{\text{eff.}}$, and $k_{\text{eff.}}$ are as above. The first equation is the same as (36a) from the Biphasic-I model. The differences of the other two equations from (36b – 36c) reflect that when the fluid velocity is sufficiently greater than the solid velocity and the viscosities are sufficiently different, the coupling between phases has weakened. In this scaling regime the two phases only communicate through the pressure gradient.

Monophasic: In the limit that the melt becomes disconnected, Biphasic-I limits to a monophasic system:

$$0 = \bar{\rho}\mathbf{g} - \nabla P + \nabla \cdot [2\mu_s(1 - \phi) e(\mathbf{V}^s) + 2\eta_{\text{eff.}}^{lm} e_{lm}(\mathbf{V}^s)] \quad (38a)$$

$$\nabla \cdot \mathbf{V}^s = 0 \quad (38b)$$

where $\eta_{\text{eff.}}$ is as above. This is an incompressible Stokes system modeling a composite material with an anisotropic viscosity.

3. Detailed Expansions and Matching Orders

This section and Appendices A–B provide the detailed derivation and expansions required to derive the Biphasic-I model summarized in Section 2.4. The other two models are derived in Appendix C. This material is admittedly technical but we want to provide sufficient information to offer a road map for related studies.

We begin by writing our equations in dimensionless form. For the scaling regimes we study, the dimensionless forms of the force equations, (11), the incompressibility equations, (5b), and the boundary conditions, (6a) and (6b), are:

$$\nabla_y \cdot [-\tilde{p}^s I + 2\epsilon^{-1} \tilde{\mu}_s e_y(\tilde{\mathbf{v}}^s)] + \epsilon \tilde{\mathbf{g}}^s = 0 \quad (39a)$$

$$\nabla_y \cdot [-\tilde{p}^f I + 2\epsilon^1 \tilde{\mu}_f e_y(\tilde{\mathbf{v}}^f)] + \epsilon \tilde{\mathbf{g}}^f = 0 \quad (39b)$$

$$\nabla_y \cdot \tilde{\mathbf{v}}^s = 0 \quad (39c)$$

$$\nabla_y \cdot \tilde{\mathbf{v}}^f = 0 \quad (39d)$$

$$[-\tilde{p}^s I + 2\epsilon^{-1} \tilde{\mu}_s e_y(\tilde{\mathbf{v}}^s)] \cdot \mathbf{n} = [-\tilde{p}^f I + 2\epsilon^1 \tilde{\mu}_f e_y(\tilde{\mathbf{v}}^f)] \cdot \mathbf{n} \quad (39e)$$

$$\tilde{\mathbf{v}}^s = \mathcal{V} \tilde{\mathbf{v}}^f \quad (39f)$$

All dependent variables are functions of both \mathbf{x} and \mathbf{y} . Periodicity in \mathbf{y} is imposed to capture the periodicity of the microstructure. Derivatives act on both arguments,

$$\boxed{\frac{\partial}{\partial y_i} \mapsto \frac{\partial}{\partial y_i} + \epsilon \frac{\partial}{\partial x_i}} \quad (40)$$

Analogously, divergence, gradient, and strain rate operators become:

$$\nabla_y \cdot \mapsto \nabla_y \cdot + \epsilon \nabla_x \cdot \quad (41a)$$

$$\nabla_y \mapsto \nabla_y + \epsilon \nabla_x \quad (41b)$$

$$e_y \mapsto e_y + \epsilon e_x \quad (41c)$$

3.1. Hierarchy of Equations

Expanding all variables using Eq. (8) and applying the two scale derivatives, we arrive at two hierarchies of equations, one for each phase, which can be solved successively.

Details of these expansions are given in Appendix A. For the matrix, each iterate is:

$$O(\epsilon^n) : \quad \nabla_y \cdot \sigma^{s(n)} + \nabla_x \cdot \sigma^{s(n-1)} + \delta_{n,1} \mathbf{g}^s = 0 \quad \text{in } Y_s \quad (42a)$$

$$O(\epsilon^{n+1}) : \quad \nabla_y \cdot \mathbf{v}^{s(n+1)} + \nabla_x \cdot \mathbf{v}^{s(n)} = 0 \quad \text{in } Y_s \quad (42b)$$

$$O(\epsilon^n) : \quad \sigma^{s(n)} \cdot \mathbf{n} = \sigma^{f(n)} \cdot \mathbf{n} \quad \text{on } \gamma \quad (42c)$$

$$\sigma^{s(n)} \equiv -p^{s(n)} I + 2\mu_s [e_x(\mathbf{v}^{s(n)}) + e_y(\mathbf{v}^{s(n+1)})] \quad (42d)$$

where $\delta_{n,1}$ is the Kronecker delta, such that gravity only acts at order $n = 1$. Gravity does not participate in the earlier iterates. Treating $\sigma^{s(n-1)}$ and $\mathbf{v}^{s(n)}$ as known, the equations can be interpreted as an inhomogeneous Stokes system for $\mathbf{v}^{s(n+1)}$ and $p^{s(n)}$. The first iterate of this system is at $n = -1$, and we set $\sigma^{s(-2)} = \mathbf{v}^{s(-1)} = \sigma^{f(-1)} = p^{s(-1)} = 0$.

We note that the above equations can be interpreted at each order as a linear system in the spirit of the linear algebra problem $\mathbf{A}\vec{x} = \vec{b}$. As with all such problems, there is a solvability condition which must be satisfied. For our system, the constraint can be interpreted as follows: to be solvable at order n , the integrated surface stress on the solid exerted by the fluid, must match the integrated force felt within in the solid,

$$\int_{\gamma} \sigma^{f(n)} \cdot \mathbf{n} dS = - \int_{Y_s} (\nabla_x \cdot \sigma^{s(n-1)} + \delta_{n,1} \mathbf{g}^s) dy. \quad (43)$$

The enforcement of (43) separates scales and steers us to the macroscopic system. This condition can be derived by integrating (42a) over Y_s , invoking the divergence theorem on the $\nabla_y \cdot \sigma^{s(n)}$ term, and applying boundary condition (42c).

Complementing the equations for the matrix is a hierarchy of equations for the melt phase:

$$O(\epsilon^{n+1}) : \quad \nabla_y \cdot \sigma^{f(n+1)} + \nabla_x \cdot \sigma^{f(n)} + \delta_{n,1} \mathbf{g}^f = 0 \quad \text{in } Y_f \quad (44a)$$

$$O(\epsilon^n) : \quad \nabla_y \cdot \mathbf{v}^{f(n)} + \nabla_x \cdot \mathbf{v}^{f(n-1)} = 0 \quad \text{in } Y_f \quad (44b)$$

$$O(\epsilon^n) : \quad \mathbf{v}^{f(n)} = \begin{cases} \mathbf{v}^{s(n)} & \text{on } \gamma \text{ if } \mathcal{V} = O(1), \\ \mathbf{v}^{s(n-1)} & \text{on } \gamma \text{ if } \mathcal{V} = O(\epsilon^{-1}). \end{cases} \quad (44c)$$

$$\sigma^{f(n)} \equiv -p^{f(n)} I + 2\mu_f (e_y(\mathbf{v}^{f(n-1)}) + e_x(\mathbf{v}^{f(n-2)})) \quad (44d)$$

As in the solid case, we treat lower order terms, $\sigma^{f(n-1)}$ and $\mathbf{v}^{f(n-2)}$ as known, then solve for pressure $p^{f(n)}$ and velocity $\mathbf{v}^{f(n-1)}$. The first iterate of this system is at $n = -1$, and we set $\sigma^{f(-1)} = \mathbf{v}^{f(-1)} = \mathbf{v}^{f(-2)} = \mathbf{v}^{s(-1)} = \mathbf{v}^{s(-2)} = 0$.

Again, there is a solvability condition. At each order, the flow of the solid at the boundary must balance the dilation or compaction of the fluid:

$$\int_{Y_f} \nabla_x \cdot \mathbf{v}^{f(n)} d\mathbf{y} = \begin{cases} - \int_{\gamma} \mathbf{v}^{s(n)} \cdot \mathbf{n} dS & \text{if } \mathcal{V} = O(1) \\ - \int_{\gamma} \mathbf{v}^{s(n-1)} \cdot \mathbf{n} dS & \text{if } \mathcal{V} = O(\epsilon^{-1}) \end{cases} \quad (45)$$

This can be derived by integrating (44b) over Y_f , invoking the divergence theorem on the $\nabla_y \cdot \mathbf{v}^{f(n)}$ term, and applying boundary condition (44c). Both solvability conditions (43) and (45) will be essential for developing macroscopic effective media equations.

3.2. Leading Order Equations

The leading order equations are the same in the three scaling regimes we examine. From (42a), (42b), (42c), and (44a), the leading equations are:

$$O(\epsilon^{-1}) : \quad \nabla_y \cdot \sigma^{s(-1)} = 0 \quad \text{in } Y_s \quad (46a)$$

$$O(\epsilon^0) : \quad \nabla_y \cdot \mathbf{v}^{s(0)} = 0 \quad \text{in } Y_s \quad (46b)$$

$$O(\epsilon^0) : \quad \nabla_y \cdot \sigma^{f(0)} = 0 \quad \text{in } Y_f \quad (46c)$$

$$O(\epsilon^{-1}) : \quad \sigma^{s(-1)} \cdot \mathbf{n} = 0 \quad \text{on } \gamma \quad (46d)$$

214 These equations can be solved analytically to show that the leading order matrix velocity
215 and melt pressure are independent of the fine scale.

To solve for the leading order solid velocity $\mathbf{v}^{s(0)}$, note that the solid stress is $\sigma^{s(-1)} = 2\mu_s e_y(\mathbf{v}^{s(0)})$ from (42d) and multiply (46a) by $\mathbf{v}^{s(0)}$ and integrate by parts over Y_s ,

$$\begin{aligned} & \int_{Y_s} \partial_{y_j} v_i^{s(0)} \sigma_{ij}^{s(-1)} d\mathbf{y} \\ &= \int_{\gamma} v_i^{s(0)} \sigma_{ij}^{s(-1)} n_j dS - 2\mu_s \int_{Y_s} |e_y(\mathbf{v}^{s(0)})|^2 d\mathbf{y} = 0 \end{aligned}$$

Applying the boundary condition (46d), we obtain

$$\int_{Y_s} |e_y(\mathbf{v}^{s(0)})|^2 d\mathbf{y} = 0.$$

which implies that $\mathbf{v}^{s(0)}$ is constant in \mathbf{y} ,

$$\mathbf{v}^{s(0)} = \mathbf{v}^{s(0)}(\mathbf{x}) \quad (47)$$

216 $\mathbf{v}^{s(0)}$ automatically satisfies (46b).

Turning to the fluid, the fluid stress is given by (44d) as $\sigma^{f(0)} = -p^{f(0)}I$, thus (46c) becomes,

$$\nabla_y \cdot \sigma^{f(0)} = \nabla_y \cdot (-p^{f(0)}I) = -\nabla_y p^{f(0)} = 0.$$

which implies,

$$p^{f(0)} = p^{f(0)}(\mathbf{x}). \quad (48)$$

3.3. Successive Orders in the Solid Phase

At the next order ($n = 0$) in (42a–42c),

$$O(\epsilon^0) : \quad \nabla_y \cdot \sigma^{s(0)} = 0 \quad \text{in } Y_s \quad (49a)$$

$$O(\epsilon^1) : \quad \nabla_x \cdot \mathbf{v}^{s(0)} + \nabla_y \cdot \mathbf{v}^{s(1)} = 0 \quad \text{in } Y_s \quad (49b)$$

$$O(\epsilon^0) : \quad \sigma^{s(0)} \cdot \mathbf{n} = \sigma^{f(0)} \cdot \mathbf{n} \quad \text{on } \gamma \quad (49c)$$

From (42d),

$$\sigma^{s(0)} \equiv -p^{s(0)} I + 2\mu_s (e_y(\mathbf{v}^{s(1)}) + e_x(\mathbf{v}^{s(0)}))$$

Solvability condition (43) on the stresses is satisfied because $p^{f(0)} = p^{f(0)}(\mathbf{x})$ yielding

$$\int_{\Gamma} (-p^{f(0)} I) \cdot \mathbf{n} = 0.$$

It is helpful to define the pressure difference between solid and fluid as $q = p^{s(0)} - p^{f(0)}$.

$\mathbf{v}^{s(1)}$ and q solve

$$\nabla_y \cdot (-qI + 2\mu_s e_y(\mathbf{v}^{s(1)})) = 0 \quad \text{in } Y_s \quad (50a)$$

$$\nabla_y \cdot \mathbf{v}^{s(1)} = -\nabla_x \cdot \mathbf{v}^{s(0)} \quad \text{in } Y_s \quad (50b)$$

$$(-qI + 2\mu_s e_y(\mathbf{v}^{s(1)})) \cdot \mathbf{n} = (-2\mu_s e_x(\mathbf{v}^{s(0)})) \cdot \mathbf{n} \quad \text{on } \gamma \quad (50c)$$

This is an inhomogeneous Stokes problem with the forcing terms $\nabla_x \cdot \mathbf{v}^{s(0)}$ in (50b) and $2\mu_s e_x(\mathbf{v}^{s(0)}) \cdot \mathbf{n}$ in (50c); all forcing terms are independent of \mathbf{y} . Because the problem is linear, we can solve for each component of the forcing independently. The complete

solution is the superposition:

$$\mathbf{v}^{s(1)} = 2e_{x,lm}(\mathbf{v}^{s(0)})\bar{\chi}^{lm} - (\nabla_x \cdot \mathbf{v}^{s(0)})\bar{\xi} \quad (51)$$

$$q = p^{s(0)} - p^{f(0)} = 2\mu_s e_{x,lm}(\mathbf{v}^{s(0)})\pi^{lm} - \mu_s (\nabla_x \cdot \mathbf{v}^{s(0)})\zeta \quad (52)$$

Summation over lm is implied. For each ordered pair (l, m) , there is a velocity, $\bar{\chi}^{lm}$, and pressure, π^{lm} , contributed from the corresponding component of the surface stress on the solid, $2e_{x,lm}(\mathbf{v}^{s(0)})$. The velocity $\bar{\xi}$ and pressure ζ arise from the dilation/compaction forcing. $\bar{\chi}^{lm}$, π^{lm} , $\bar{\xi}$, and ζ are defined in Table 6 and full statements of the cell problems are given in Appendix B. These solve the aforementioned auxiliary, or cell, problems, which are Stokes boundary value problems posed on Y_s .

Cell problems may be interpreted as the unit response of the medium to a particular forcing. For generic three-dimensional cell geometries, the cell problems lack clear analytic solutions, and one must resort to numerical computation to understand them. In our second paper, we survey them numerically.

We make two observations on (52). First, it agrees with models that permit the pressures to be unequal, as in *Scott and Stevenson* [1984]; *Stevenson and Scott* [1991]; *Bercovici et al.* [2001a]; *Bercovici and Ricard* [2003]. It also makes clear that the question of whether there are one or two pressures in macroscopic models of partial melts is entirely semantic. There are two pressures, but to leading order each can be expressed in terms of the other. Second, it captures that part of any pressure jump is due to the macroscopic compaction of the matrix. Such a relation was also discussed in *Spiegelman et al.* [2007]; *Katz et al.* [2007].

3.4. Macroscopic Force Balance in the Matrix

Though we have solved for $\mathbf{v}^{s(1)}$, $p^{s(0)}$ in terms of $\mathbf{v}^{s(0)}$ and $p^{f(0)}$, we still do not have a macroscopic equation relating velocity and pressure. To find such an equation we go to the next order of equations for the matrix and use the solvability condition, (43), to constrain them. This constraint becomes our macroscopic equation; we do not actually solve for $\mathbf{v}^{s(2)}$ and $p^{s(1)}$.

At the next order of (42a–42c), the equations are:

$$O(\epsilon^1) : \quad \nabla_x \cdot \sigma^{s(0)} + \nabla_y \cdot \sigma^{s(1)} + \mathbf{g}^s = 0 \quad \text{in } Y_s \quad (53a)$$

$$O(\epsilon^2) : \quad \nabla_x \cdot \mathbf{v}^{s(1)} + \nabla_y \cdot \mathbf{v}^{s(2)} = 0 \quad \text{in } Y_s \quad (53b)$$

$$O(\epsilon^1) : \quad \sigma^{s(1)} \cdot \mathbf{n} = \sigma^{f(1)} \cdot \mathbf{n} \quad \text{on } \gamma \quad (53c)$$

$\sigma^{s(1)}$ is given by (42d):

$$\sigma^{s(1)} = -p^{s(1)} + 2\mu_s [e_x(\mathbf{v}^{s(1)}) + e_y(\mathbf{v}^{v(2)})] \quad (54)$$

According to our force matching solvability condition (43),

$$\int_{\gamma} \sigma^{f(1)} \cdot \mathbf{n} dS = - \int_{Y_s} (\nabla_x \cdot \sigma^{s(0)} + \mathbf{g}^s) d\mathbf{y} \quad (55)$$

By stress boundary condition (53c), $\sigma^{s(1)} \cdot \mathbf{n} = \sigma^{f(1)} \cdot \mathbf{n}$ on γ , so

$$\begin{aligned} \int_{Y_s} (\nabla_x \cdot \sigma^{s(0)} + \mathbf{g}^s) d\mathbf{y} &= - \int_{\gamma} \sigma^{f(1)} \cdot \mathbf{n} dS \\ &= \int_{Y_f} \nabla_y \cdot \sigma^{f(1)} d\mathbf{y} \end{aligned} \quad (56)$$

Using fluid momentum equation (44a), $\nabla_y \cdot \sigma^{f(1)} = -\nabla_x \cdot \sigma^{f(0)} - \mathbf{g}^f$ in Y_f , hence

$$\begin{aligned} \int_{Y_s} (\nabla_x \cdot \sigma^{s(0)}) d\mathbf{y} + \int_{Y_f} (\nabla_x \cdot \sigma^{f(0)}) d\mathbf{y} \\ + (1 - \phi) \mathbf{g}^s + \phi \mathbf{g}^f = 0 \end{aligned} \quad (57)$$

Commuting the integration and divergence operators,

$$\begin{aligned}
& -\nabla_x [\langle p^{s(0)} \rangle_s + \langle p^{f(0)} \rangle_f] \\
& + 2\mu_s \nabla_x \cdot [\langle e_x(\mathbf{v}^{s(0)}) \rangle_s + \langle e_y(\mathbf{v}^{s(1)}) \rangle_s] \\
& + \bar{\rho} \mathbf{g} = 0
\end{aligned} \tag{58}$$

where angle brackets $\langle \cdot \rangle_s$ denote volume averages over the solid domain Y_s (likewise $\langle \cdot \rangle_f$ over Y_f). If we substitute (51) and (52) for $p^{s(0)}$ and $\mathbf{v}^{s(1)}$, then

$$\begin{aligned}
0 = & \bar{\rho} \mathbf{g} - \nabla_x p^{f(0)} \\
& - \nabla_x \{ 2\mu_s e_{x,lm}(\mathbf{v}^{s(0)}) \langle \pi^{lm} \rangle_s - \mu_s \langle \zeta \rangle_s \nabla_x \cdot \mathbf{v}^{s(0)} \} \\
& + 2\mu_s \nabla_x \cdot \{ (1 - \phi) e_x(\mathbf{v}^{s(0)}) + 2e_{x,lm}(\mathbf{v}^{s(0)}) \langle e_y(\bar{\chi}^{lm}) \rangle_s \} \\
& - 2\mu_s \nabla_x \cdot \{ \langle e_y(\bar{\xi}) \rangle_s \nabla_x \cdot \mathbf{v}^{s(0)} \}
\end{aligned} \tag{59}$$

We now have an equation for $\mathbf{v}^{s(0)}$ and $p^{f(0)}$, both functions of \mathbf{x} . Multiplying this equation by P^s/L restores dimensions. Again, we note that we did not solve (53a–53c). (59) is merely the equation that must be satisfied for (53a–53c) to satisfy momentum compatibility condition (43).

3.5. Macroscopic Force Balance in the Fluid

We now seek macroscopic equations for the melt. As in the case of the solid, we must iterate out to the second order correction and use the solvability condition to obtain a macroscopic equation.

We first solve for the first correction, obtaining $\mathbf{v}^{f(0)}$ and $p^{f(1)}$, and average them. From the hierarchy of fluid equations, (44a – 44d), the fluid equations at this order are

$$O(\epsilon^1) : \quad \nabla_x \cdot \sigma^{f(0)} + \nabla_y \cdot \sigma^{f(1)} + \mathbf{g}^f = 0 \quad \text{in } Y_f \tag{60}$$

$$O(\epsilon^0) : \quad \nabla_y \cdot \mathbf{v}^{f(0)} = 0 \quad \text{in } Y_f \tag{61}$$

with stress

$$\sigma^{f(1)} = -p^{f(1)}I + 2\mu_f e_y(\mathbf{v}^{f(0)})$$

and boundary conditions

$$\mathbf{v}^{f(0)} = \begin{cases} \mathbf{v}^{s(0)} & \text{on } \gamma \text{ if } \mathcal{V} = O(1) \\ 0 & \text{on } \gamma \text{ if } \mathcal{V} = O(\epsilon^{-1}) \end{cases} \quad (62)$$

One of the most relevant scaling regimes for magma migration is Biphasic-I with $\mathcal{V} = O(1)$ and $\mathcal{M} = O(\epsilon^2)$, summarized in Section 2.4. We derive it here. The two other systems, Biphasic-II and Monophasic, are similar and presented in Appendix C.

If we substitute the stresses $\sigma^{f(0)}$ and $\sigma^{f(1)}$ into (60 – 61), we have

$$\begin{aligned} -\nabla_x p^{f(0)} - \nabla_y p^{f(1)} + \mu_f \nabla_y^2 \mathbf{v}^{f(0)} + \mathbf{g}^f &= 0 \quad \text{in } Y_f \\ \nabla_y \cdot \mathbf{v}^{f(0)} &= 0 \quad \text{in } Y_f \end{aligned}$$

with boundary condition $\mathbf{v}^{f(0)} = \mathbf{v}^{s(0)}$ on γ . Recall that $p^{f(0)}$, $\mathbf{v}^{s(0)}$, and \mathbf{g}^f are interpreted as known, inhomogeneous, \mathbf{y} independent quantities forcing $\mathbf{v}^{f(0)}$ and $p^{f(1)}$. Since it is easier to solve a problem with homogeneous boundary conditions, we define $\mathbf{w} \equiv \mathbf{v}^{f(0)} - \mathbf{v}^{s(0)}$, simplifying the above equations into

$$-\nabla_y p^{f(1)} + \mu_f \nabla_y^2 \mathbf{w} = \nabla_x p^{f(0)} - \mathbf{g}^f \quad \text{in } Y_f \quad (63a)$$

$$\nabla_y \cdot \mathbf{w} = 0 \quad \text{in } Y_f \quad (63b)$$

$$\mathbf{w} = 0 \quad \text{on } \gamma \quad (63c)$$

This is the classic homogenization problem of flow in a rigid porous medium and leads to Darcy's Law. It is discussed in many of the cited texts on homogenization, particularly *Hornung* [1997].

The volume compatibility condition (45) is trivially satisfied since $\mathbf{w}|_\gamma = 0$,

$$0 = \int_{Y_f} (\nabla_y \cdot \mathbf{w}) d\mathbf{y} = \int_\gamma \mathbf{w} \cdot \mathbf{n} dS = 0.$$

As in the case of the solid phase, we solve (63a)–(64c) via cell problems, taking advantage of the linearity of the problem. We decompose the right hand side forcing terms in (63a) into \mathbf{e}_1 , \mathbf{e}_2 and \mathbf{e}_3 components, solving in each coordinate, then forming the superposition of the three to get the solution. Let q^i , \mathbf{k}^i be \mathbf{y} periodic functions solving:

$$-\nabla_y q^i + \nabla_y^2 \mathbf{k}^i = -\mathbf{e}_i \quad \text{in } Y_f \quad (64a)$$

$$\nabla_y \cdot \mathbf{k}^i = 0 \quad \text{in } Y_f \quad (64b)$$

$$\mathbf{k}^i = 0 \quad \text{on } \gamma \quad (64c)$$

\mathbf{e}_i is the unit vector in the i -th direction. These problems thus measure the unit response of the fluid to such a forcing. Using the solutions,

$$\mathbf{w} = -\frac{1}{\mu_f} \mathbf{k}^i \left(\partial_{x_i} p^{f(0)} - g_i^f \right) \quad (65)$$

$$p^{f(1)}(\mathbf{x}, \mathbf{y}) = -q^i \left(\partial_{x_i} p^{f(0)} - g_i^f \right) \quad (66)$$

Averaging over Y_f , we get the macroscopic equation for the fluid,

$$\langle \mathbf{v}^{f(0)} \rangle_f - \phi \mathbf{v}^{s(0)} = -\frac{\langle K \rangle_f}{\mu_f} (\nabla_x p^{f(0)} - \mathbf{g}^f) \quad (67)$$

This is Darcy's Law with buoyancy and in a moving frame. $\langle K \rangle_f$ is the permeability tensor. K is the matrix, or alternatively the second order tensor,

$$K = [\mathbf{k}^1 \quad \mathbf{k}^2 \quad \mathbf{k}^3] \quad (68)$$

and

$$\langle K \rangle_f = \left[\int_{Y_f} \mathbf{k}^1 d\mathbf{y} \quad \int_{Y_f} \mathbf{k}^2 d\mathbf{y} \quad \int_{Y_f} \mathbf{k}^3 d\mathbf{y} \right] \quad (69)$$

While the leading order solid velocity is \mathbf{y} -independent, the leading order fluid velocity remains sensitive to the fine scale. For a macroscopic description, it can only be defined as an average flux; this is the Darcy velocity of the fluid.

This is not yet a closed system. Advancing to the next order of (44a – 44c), we have

$$O(\epsilon^2) : \quad \nabla_x \cdot \sigma^{f(1)} + \nabla_y \cdot \sigma^{f(2)} = 0 \quad \text{in } Y_f \quad (70)$$

$$O(\epsilon^1) : \quad \nabla_x \cdot \mathbf{v}^{f(0)} + \nabla_y \cdot \mathbf{v}^{f(1)} = 0 \quad \text{in } Y_f \quad (71)$$

$$O(\epsilon^1) : \quad \mathbf{v}^{f(1)} = \mathbf{v}^{s(1)} \quad \text{on } \gamma \quad (72)$$

The solution must satisfy the volume compatibility condition (45),

$$\int_{Y_f} \nabla_x \cdot \mathbf{v}^{f(0)} = - \int_{\gamma} \mathbf{v}^{s(0)} \cdot \mathbf{n} dS = 0 \quad (73)$$

Combining this with (49b), we get

$$\nabla_x \cdot [\langle \mathbf{v}^{f(0)} \rangle_f + (1 - \phi) \mathbf{v}^{s(0)}] = 0 \quad (74)$$

This is a macroscopic volume compatibility condition. Equations (59), (67), and (74) now form a closed system. Dimensions may be restored to (67) by multiplying by V^f and (74) by V^f/L ; a factor of ℓ^2 will appear in front of $\langle K \rangle_f$, as expected.

3.6. Symmetry Simplifications

The macroscopic equations can be simplified if we assume that the cell geometry is symmetric with respect to both reflections about the principal axes and rigid rotations. Though this is a further idealization, the equations retain their essential features.

Under these two assumptions, (67) (for Biphasic I) and (C1) (for Biphasic II) are

$$\langle \mathbf{v}^{f(0)} \rangle_f - \phi \mathbf{v}^{s(0)} = - \frac{k_{\text{eff.}}}{\mu_f} (\nabla_x p^{f(0)} - \mathbf{g}^f) \quad (75)$$

$$\langle \mathbf{v}^{f(0)} \rangle_f = - \frac{k_{\text{eff.}}}{\mu_f} (\nabla_x p^{f(0)} - \mathbf{g}^f) \quad (76)$$

(59) becomes

$$0 = \bar{\rho} \mathbf{g} - \nabla_x p^{f(0)} + \nabla_x \left[\left(\zeta_{\text{eff.}} - \frac{2}{3} \mu_s (1 - \phi) \right) \nabla_x \cdot \mathbf{v}^{s(0)} \right] + \nabla_x \cdot \left[2(1 - \phi) \mu_s e_x(\mathbf{v}^{s(0)}) + 2\eta_{\text{eff.}}^{lm} e_{x,lm}(\mathbf{v}^{s(0)}) \right] \quad (77)$$

$k_{\text{eff.}}$, $\zeta_{\text{eff.}}$, and $\eta_{\text{eff.}}$ are defined in terms of the solutions of the cell problems:

$$k_{\text{eff.}} = \langle K_{11} \rangle_f \quad (78)$$

$$\zeta_{\text{eff.}} = \mu_s \langle \zeta \rangle_s - \frac{2}{3} \mu_s (1 - \phi) \quad (79)$$

$$\eta_{\text{eff.}}^{lm} = 2\mu_s \langle e_y(\bar{\chi}^{lm}) \rangle_s \quad (80)$$

$\eta_{\text{eff.}}$ is a fourth order tensor. It is a supplementary viscosity, capturing the grain scale anisotropy of the cell domain. With these symmetry reductions, there are now only four material parameters to be solved for: $\langle K_{11} \rangle_f$, $\langle \zeta \rangle_s$, $\langle e_{y,11}(\bar{\chi}^{11}) \rangle_s$, and $\langle e_{y,12}(\bar{\chi}^{12}) \rangle_s$ corresponding to the macroscopic permeability, bulk viscosity and two effective components of an anisotropic viscosity. Additional details of the symmetry simplifications may be found in Appendix E.

If we now define $\mathbf{V}^s \equiv \mathbf{v}^{s(0)}$, $\mathbf{V}^f \equiv \langle \mathbf{v}^{f(0)} \rangle_f / \phi$, and $P \equiv p^{f(0)}$, and drop the x subscripts from the derivatives, the above equations become (36a – 36c) presented in Section 2.4.

4. Discussion

We have successfully used homogenization to derive three macroscopic models for conservation of momentum in partially molten systems. We now consider these models further, compare them with previous models derived using multiphase flow methods and discuss some caveats and future directions.

4.1. Remarks on Homogenization Models

The differences amongst the three models of Section 2.4 arise from the assumptions on two dimensionless numbers, \mathcal{V} and \mathcal{M} , and the microstructure. All three rely on the additional assumptions that $Q_\ell^f = O(\epsilon)$ and $\mathcal{P} = O(1)$. It is helpful to write the three models as a unified set of equations:

$$0 = \bar{\rho}\mathbf{g} - \nabla P + \nabla \left[\left(\zeta_{\text{eff.}} - \frac{2}{3}\mu_s(1 - \phi) \right) \nabla \cdot \mathbf{V}^s \right] \quad (81a)$$

$$+ \nabla \cdot [2(1 - \phi)\mu_s e(\mathbf{V}^s) + 2\eta_{\text{eff.}}^{lm} e_{lm}(\mathbf{V}^s)]$$

$$\phi(\mathbf{V}^f - \mathcal{V}^{-1}\mathbf{V}^s) = -\frac{k_{\text{eff.}}}{\mu_f} (\nabla P + \mathbf{g}^f) \quad (81b)$$

$$\nabla \cdot [\phi\mathbf{V}^f + \mathcal{V}^{-1}(1 - \phi)\mathbf{V}^s] = 0 \quad (81c)$$

As \mathcal{V} varies from $O(\epsilon^0)$ to $O(\epsilon^{-1})$, we transition between Biphasic-I and Biphasic-II. Letting the pore network disconnect, $k_{\text{eff.}} \rightarrow 0$. Consequently, $\mathbf{V}^f \rightarrow \mathcal{V}^{-1}\mathbf{V}^s$ in (81b). This recovers macroscopic incompressibility in (81c), $\nabla \cdot \mathbf{V}^s = 0$. The divergence terms also drop from the matrix force balance equation. Making rigorous mathematical sense of the transition between the connected and disconnected pore network is an important open problem. It is also interesting that the scalings do not fully describe the macroscopic equations; the grain scale structure can play a role.

We return to our motivating problem, partially molten rock in the asthenosphere. As we saw in Section 2.3, for a given ϵ , the parameters \mathcal{V} and \mathcal{M} include a range where a macroscopic description is possible. We lose our ability to homogenize when either $\mathcal{M}\mathcal{V} \gg \epsilon^2$ or $\mathcal{M}\mathcal{V} \ll \epsilon^2$. There may be interesting transitions here. That the two parameters must be related by $\mathcal{M}\mathcal{V} = O(\epsilon^2)$ would seem a serious constraint on this approach and its applicability; however, this has another interpretation.

The condition on \mathcal{MV} stipulates that the length scales, viscosities, and velocities, be related by

$$L = \ell \sqrt{\frac{\mu_s}{\mu_f} \frac{V^s}{V^f}} \quad (82)$$

This also assumes $\mathcal{P} = O(1)$. This can be reinterpreted as the macroscopic length scale on which, given the viscosities and characteristic velocities of a partially molten mix we should *expect* to observe a biphasic, viscously deformable, porous media. Based on our estimates on the viscosities, velocities, and grain scale in Table 3,

$$L \approx 10^{-1} - 10^5 \text{ km} \quad (83)$$

Length (82) is similar, but not identical to the compaction length of *McKenzie* [1984],

$$\delta_{\text{M84}} = \sqrt{\frac{\kappa(1-\phi)(\zeta_s + \frac{4}{3}\mu_s)}{\mu_f}} \quad (84)$$

The general scaling is similar as $\kappa \propto \ell^2$ therefore the leading scaling is $\ell \sqrt{\mu_s/\mu_f}$. Nevertheless δ_{M84} is porosity dependent through both permeability, κ and the viscosities, ζ_s and μ_s , making it dynamically and spatially varying. To understand the variation in compaction length, it is critical to calculate both permeabilities and viscosities that are consistent with the underlying microstructure. Homogenization provides this computational machinery through the cell problems. The companion paper calculates consistent constitutive relations for several simple pore microstructures and suggests that in the limit $\phi \rightarrow 0$, $\delta_{\text{M84}} \rightarrow 0$ which has important implications for the transition to melt-free regions. However, L is not a substitute for δ_{M84} ; such a subsidiary length scale may also appear.

Under the assumption that $\mathcal{V} = O(1)$, (82) also bears resemblance to the compaction length of *Ricard et al.* [2001],

$$\delta_{\text{BRS01}} = \sqrt{\frac{\kappa_0 \mu_s}{\mu_f}} \quad (85)$$

κ_0 is a geometric prefactor in a power law scalar permeability relationship $\kappa = \kappa_0 \phi^n$ and $\kappa_0 \propto \ell^2$.

4.2. Comparison with Existing Models

There are several interesting and important differences between our results and previous models derived using multiphase flow methods. Most fundamental is that we begin with a grain scale model, assume certain scalings, and formally derive a macroscopic model. The anticipated constitutive laws also emerge from these assumptions.

In the limit of large viscosity variations, the conservation of momentum equations in previous models can be closely identified with the Biphasic-I model, where $\mathcal{V} = O(1)$ and $\mathcal{M} = O(\epsilon^2)$, given by equations (36a – 36c), providing some validation. Compare with *McKenzie* [1984],

$$\partial_t (\rho_f \phi) + \nabla \cdot (\rho_f \phi \mathbf{V}^f) = \text{mass transfer} \quad (86a)$$

$$\partial_t [\rho_s (1 - \phi)] + \nabla \cdot [\rho_s (1 - \phi) \mathbf{V}^s] = -\text{mass transfer} \quad (86b)$$

$$\phi (\mathbf{V}^f - \mathbf{V}^s) = -\frac{\kappa}{\mu_f} (\nabla P - \mathbf{g}^f) \quad (86c)$$

$$0 = \bar{\rho} \mathbf{g} - \nabla P + \nabla \cdot [2(1 - \phi) \mu_s e(\mathbf{V}^s)] + \nabla \cdot \left[(1 - \phi) \left(\zeta_s - \frac{2}{3} \mu_s \right) \nabla \cdot \mathbf{V}^s \right] \quad (86d)$$

κ , μ_s , and ζ_s are the permeability, shear viscosity, and bulk viscosity, which have unspecified dependencies on porosity. We have reused the symbols \mathbf{V}^f , \mathbf{V}^s , and P , to denote the macroscopic fluid and solid velocities, and pressure.

In the absence of melting and freezing, there is good agreement between the two models if we make the identifications $\zeta_{\text{eff.}} \equiv \zeta_s$ and $k_{\text{eff.}} \equiv \kappa$. The main difference is the appearance of $\eta_{\text{eff.}}$ term in (36a), reflecting our consideration of a microstructure. We emphasize that

308 this macroscopic anisotropy is geometric in origin; the grain scale model was isotropic in
 309 each phase.

Now we compare with *Bercovici and Ricard* [2003], in the “geologically relevant limit” described by the authors in their Section 3.1. With a bit of algebra, and using our notation, this can be written as:

$$\partial_t \phi + \nabla \cdot (\phi \mathbf{V}^f) = 0 \quad (87a)$$

$$\partial_t (1 - \phi) + \nabla \cdot [(1 - \phi) \mathbf{V}^s] = 0 \quad (87b)$$

$$\phi(\mathbf{V}^f - \mathbf{V}^s) = -\frac{\kappa}{\mu_f}(\nabla P - \mathbf{g}^f) \quad (87c)$$

$$0 = \bar{\rho} \mathbf{g} - \nabla P + \nabla \cdot [2(1 - \phi)\mu_s e(\mathbf{V}^s)] + \nabla \cdot \left[(1 - \phi) \left(\mu_s \frac{C_0}{\phi} - \frac{2}{3} \mu_s \right) \nabla \cdot \mathbf{V}^s \right] \\ + \nabla (\text{surface energy and damage}) \quad (87d)$$

310 In this model, C_0 is a dimensionless, $O(1)$ constant. The surface energy and damage
 311 terms, which we have not reproduced, capture surface physics and grain deformation. In
 312 the absence of these physics, there is again good agreement between Biphasic-I and this
 313 model if we make the identifications $\zeta_{\text{eff.}} \equiv \mu_s C_0 \phi^{-1}$ and $k_{\text{eff.}} \equiv \kappa$. As with the McKenzie
 314 model, the principal difference comes from the $\eta_{\text{eff.}}$ term. *Bercovici and Ricard* [2003]
 315 noted that if one eliminates mass transfer in (86a – 86d) and surface physics from (87a –
 316 87d), the two models are identical subject to the identification $\zeta_s \equiv \mu_s C_0 \phi^{-1}$.

317 The microscale model we homogenized, assuming only fluid dynamical coupling between
 318 the phases, was sufficient to generate macroscopic equations consistent with previous
 319 models in the absence of grain-scale surface energies. An important open problem is to
 320 find a grain scale model amenable to homogenization, that includes grain scale diffusion.
 321 One might then see a consistent macroscopic manifestation of these physics, which could

be compared to models that have already attempted to included them [e.g., *Ricard and Bercovici*, 2003; *Hier-Majumder et al.*, 2006].

As mentioned previously, an advantage of the homogenization derivation over the multiphase flow derivation is that there is not the same need for closures. In other models, one may posit and then seeks closures for permeability, bulk viscosity, shear viscosity, and interphase force. These parameters might be constrained by other information; however, this will not yield an inherently self-consistent model. One particularly difficult closure is the interphase force, the force that one phase exerts on the other. The interphase force, which is a macroscopic re-expression of the melt-matrix boundary conditions, is poorly constrained and non-unique. Indeed, the model in *Bercovici et al.* [2001a], using one interphase force could not replicate the model of *McKenzie* [1984]. An equally valid interphase force led to (87a – 87d). As noted, taking out the additional physics, this agrees with (86a–86d). Though this a desirable result, the non-uniqueness of the terms remains an issue.

4.3. Some Caveats

Homogenization provides a more rigorous method for derivation of macroscopic equations as well as a clear mechanism for computing critical closures. Nevertheless, it is not foolproof and includes its own set of assumptions whose consequences need to be understood.

For example, if the cell domains of Section 2.1 are independent of \mathbf{x} , then the porosity is constant:

$$\phi = \int_{Y_f} 1 d\mathbf{y}.$$

But a perfectly periodic microstructure is unrealistic. Furthermore, once motion begins, the interface moves, likely breaking the periodic structure. If the domains do have \mathbf{x} dependence, $Y_f = Y_f(\mathbf{x})$, then we can have $\phi = \phi(\mathbf{x})$. This introduces technical difficulties in (53a), as additional terms for gradients with respect to the domain should now appear. See Appendix F for details.

A similar omission has been made in the poro-elastic literature [see *Lee and Mei*, 1997a, b, c; *Lee*, 2004, for a discussion]. As the elastic matrix deforms, the interface moves, changing the cell geometry. Earlier work *Auriault* [1991a]; *Hornung* [1997]; *Mei and Auriault* [1989] implicitly assumed that this deformation was small compared to the grain scale and could be ignored. This issue also bedevils the sintering and metallurgy papers *Auriault et al.* [1992] and *Geindreau and Auriault* [1999]. In high temperature, texturally equilibrated systems as might be expected in the asthenosphere, grain-boundary surface forces may help to maintain the geometry of the micro-structure even during large deformations. However, a consistent homogenization would need to include these additional microscale processes.

Despite this obstacle, our equations are still of utility in several ways. The first is that they are a macroscopic description of a constant porosity piece of material. Such a description has not been rigorously derived before for partially molten rock. It also acts as a tool for verifying the multiphase flow models. Taking ϕ to be instantaneously uniform, such a model should reduce to our equations. Under simplifications, the other models, such as *McKenzie* [1984]; *Bercovici and Ricard* [2003], are in agreement, up to the η_{eff} expression.

Another interpretation is that our models are valid when porosity varies sufficiently slowly. Under such an assumption, the omitted terms would be higher order in ϵ and could be justifiably dropped. There is a certain appeal to this; it would not make sense to discuss the homogenization of a material in which there were tremendous contrasts in the porosity over short length scales. Moreover, the typical porosity is $O(1\%)$, so that if the porosity parameter were also scaled, these terms may indeed be small. Such assumptions of slowly varying porosity underly all of the multiphase flow derivations (and general continuum mechanics approaches).

Our final interpretation is that the equations are part of a hierarchical model for partial melts. If we ignore melting and assume constant densities, conservation of mass can be expressed as

$$\partial_t (1 - \phi) + \nabla \cdot [(1 - \phi) \mathbf{V}^s] = 0 \quad (88)$$

We might then assume that the grain matrix may be approximated by some periodic structure at each instant. This is consistent with observations. Although the matrix deforms viscously, it retains a granular structure. Our equations are then treated as the macroscopic force balances to determine \mathbf{V}^s , and the system evolves accordingly.

Another issue with the homogenization approach is that though it illuminates how the effective viscosities and the permeability arise through the cell problems, calculating the relationship between ζ_{eff} , η_{eff} , and k_{eff} and the microstructure (e.g. porosity), requires numerically solving the cell problems. The companion paper, *Simpson et al.* [2008b], explores this, calculating effective constitutive relationships for several idealized pore geometries.

4.4. Open Problems

There are several ways this work might be extended. A natural continuation is to model the partial melt as a random medium. This might more realistically model the pore structure of rocks. The equations for upscaling could also be augmented by giving the matrix a nonlinear rheology, as in *Auriault et al.* [1992]; *Geindreau and Auriault* [1999]. This may be particularly important for magma migration; a nonlinear matrix rheology was needed to computationally model physical experiments for shear bands in *Katz et al.* [2006] and in general, non-linear power-law rheologies are expected in the dislocation creep regime [e.g., *Hirth and Kohlstedt*, 1995b].

Important mechanisms absent from these equations are surface physics which. In a fluid dynamical description, these might take the form as surface tension and diffusional terms. Such terms were posited in the models of *Ricard et al.* [2001]; *Hier-Majumder et al.* [2006]; *Bercovici and Ricard* [2005, 2003]; *Bercovici et al.* [2001b, a], but it remains to be shown how such terms in the macroscopic equations might arise consistently from microscopic physics that includes grain-scale diffusion and/or mass transfer.

The most serious question remains how to properly study a medium with macroscopic and time dependent variations in the structure. This would have implications for the many physical phenomena that also have *evolving microstructures*. Recent work in *Peter* [2007a, b, 2009] on reaction-diffusion systems in porous media may be applicable.

Appendix A: Details of the Expansions

The multiple scale expansions of (8) are applied to \tilde{p}^s , \tilde{p}^f , $\tilde{\mathbf{v}}^s$, $\tilde{\mathbf{v}}^f$ and substituted into the dimensionless equations (39a – 39f), along with the two scale derivatives, (41a – 41c).

Dropping tildes, both melt and matrix strain rate tensors expand as:

$$\begin{aligned} e_y(\mathbf{v}) &\mapsto \epsilon^0 [e_y(\mathbf{v}^{(0)})] + \epsilon^1 [e_x(\mathbf{v}^{(0)}) + e_y(\mathbf{v}^{(1)})] + \epsilon^2 [e_x(\mathbf{v}^{(1)}) + e_y(\mathbf{v}^{(2)})] + \dots \\ &\equiv \epsilon^0 e^{(0)} + \epsilon^1 e^{(1)} + \epsilon^2 e^{(2)} + \dots \end{aligned} \quad (\text{A1})$$

The stress tensors become:

$$\begin{aligned} \sigma^s &\mapsto \epsilon^{-1} [2\mu_s e^{s(0)}] + \epsilon^0 [-p^{s(0)} I + 2\mu_s e^{s(1)}] + \epsilon^1 [-p^{s(1)} I + 2\mu_s e^{s(2)}] + \dots \\ &\equiv \epsilon^{-1} \sigma^{s(-1)} + \epsilon^0 \sigma^{s(0)} + \epsilon^1 \sigma^{s(1)} + \dots \end{aligned} \quad (\text{A2a})$$

$$\begin{aligned} \sigma^f &\mapsto \epsilon^0 [-p^{f(0)} I] + \epsilon^1 [-p^{f(1)} I + 2\mu_f e^{f(1)}] + \epsilon^2 [-p^{f(2)} I + 2\mu_f e^{f(2)}] + \dots \\ &\equiv \sigma^{f(0)} + \epsilon^1 \sigma^{f(1)} + \epsilon^2 \sigma^{f(2)} + \dots \end{aligned} \quad (\text{A2b})$$

Matching powers of ϵ in equations (A2a) and (A2b) in (39a) and (39b)

$$\begin{aligned} \epsilon^{-1} \nabla_y \cdot \sigma^{s(-1)} + \epsilon^0 (\nabla_x \cdot \sigma^{s(-1)} + \nabla_y \cdot \sigma^{s(0)}) + \epsilon^1 (\nabla_x \cdot \sigma^{s(0)} + \nabla_y \cdot \sigma^{s(1)} + \mathbf{g}^s) \\ + \dots = 0 \end{aligned} \quad (\text{A3a})$$

$$\begin{aligned} \epsilon^0 \nabla_y \cdot \sigma^{f(0)} + \epsilon^1 (\nabla_x \cdot \sigma^{f(0)} + \nabla_y \cdot \sigma^{f(1)} + \mathbf{g}^f) + \epsilon^2 (\nabla_x \cdot \sigma^{f(1)} + \nabla_y \cdot \sigma^{f(2)}) \\ + \dots = 0 \end{aligned} \quad (\text{A3b})$$

Analogously, we substitute the expansions into the incompressibility equations (39c–39d), to get

$$\begin{aligned} \epsilon^0 \nabla_y \cdot \mathbf{v}^{f(0)} + \epsilon^1 (\nabla_x \cdot \mathbf{v}^{f(0)} + \nabla_y \cdot \mathbf{v}^{f(1)}) + \dots = 0 \\ \epsilon^0 \nabla_y \cdot \mathbf{v}^{s(0)} + \epsilon^1 (\nabla_x \cdot \mathbf{v}^{s(0)} + \nabla_y \cdot \mathbf{v}^{s(1)}) + \dots = 0 \end{aligned} \quad (\text{A4})$$

397 The leading order equations of (A4), $\nabla_y \cdot \mathbf{v}^{f(0)} = 0$ and $\nabla_y \cdot \mathbf{v}^{s(0)} = 0$, reflect that at the
398 grain scale, both phases are incompressible.

Making the same power series expansions in the boundary conditions, continuity of normal stress, (39e), is

$$\epsilon^{-1} \sigma^{s(-1)} \cdot \mathbf{n} + \epsilon^0 (\sigma^{s(0)} - \sigma^{f(0)}) \cdot \mathbf{n} + \dots = 0. \quad (\text{A5})$$

When $\mathcal{V} = O(1)$, the velocity boundary condition within the cell is

$$\epsilon^0 (\mathbf{v}^{s(0)} - \mathbf{v}^{f(0)}) + \epsilon^1 (\mathbf{v}^{s(1)} - \mathbf{v}^{f(1)}) + \dots = 0 \quad \text{on } \gamma. \quad (\text{A6})$$

In this case, the velocities are matched at all orders of ϵ . If instead $\mathcal{V} = O(\epsilon^{-1})$, then

$$\begin{aligned} \epsilon^{-1} \mathbf{v}^{f(0)} + \epsilon^0 (\mathbf{v}^{f(1)} - \mathbf{v}^{s(0)}) \\ + \epsilon^1 (\mathbf{v}^{f(2)} - \mathbf{v}^{s(1)}) + \dots = 0 \quad \text{on } \gamma. \end{aligned} \tag{A7}$$

In contrast to the $\mathcal{V} = O(1)$ case, the leading order fluid velocity is independent of the solid, and there is cross coupling across orders.

Appendix B: Cell Problems in the Matrix

In general, there are two classes of cell problems associated with the matrix phase, and a total of seven cell problems. Domain symmetry can reduce the number of unique cell problems.

B1. Cell Problem for Dilation Stress on Solid

This addresses the term $\nabla_x \cdot \mathbf{v}^{s(0)}$ in (50b). This is a less common Stokes problem, with a prescribed function in the divergence equation. They are briefly discussed in *Temam* [2001]. Let $\bar{\xi}, \zeta$ be \mathbf{y} periodic functions solving

$$\nabla_y \cdot (-\zeta I + 2e_y(\bar{\xi})) = 0 \quad \text{in } Y_s \tag{B1a}$$

$$\nabla_y \cdot \bar{\xi} = 1 \quad \text{in } Y_s \tag{B1b}$$

$$(-\zeta I + 2e_y(\bar{\xi})) \cdot \mathbf{n} = 0 \quad \text{on } \gamma \tag{B1c}$$

The solution measures the response of a unit cell of the matrix to the divergence condition (B1b).

B2. Cell Problem for Surface Stresses on Solid

This problem tackles the boundary stress in (50c). Let $\bar{\chi}^{lm}$, π^{lm} be \mathbf{y} periodic functions solving

$$\nabla_y \cdot (-\pi^{lm} I + 2e_y(\bar{\chi}^{lm})) = 0 \quad \text{in } Y_s \quad (\text{B2a})$$

$$\nabla_y \cdot \bar{\chi}^{lm} = 0 \quad \text{in } Y_s \quad (\text{B2b})$$

$$(-\pi^{lm} \delta_{ij} + 2e_{y,ij}(\bar{\chi}^{lm})) n_j = -\frac{1}{2} (\delta_{il} \delta_{jm} + \delta_{im} \delta_{jl}) n_j \quad \text{on } \gamma \quad (\text{B2c})$$

406 $(\bar{\chi}^{lm}, \pi^{lm})$ measure the response of a unit cell of the matrix to a given unit surface stress,
407 depending on indices (l, m) . Observe that because the tensor on the right hand side of
408 (B2c), operating on \mathbf{n} , is symmetric, the solution to problem (l, m) is the same as the
409 solution for problem (m, l) . For general domains, there are thus six unique cell problems
410 associated with surface stress forcing.

Appendix C: Additional Scaling Regimes

411 In addition to the Biphasic-I regime which we derived in Section 3.5, we presented two
412 other cases in Section 2.4. These are Biphasic-II, where $\mathcal{V} = O(\epsilon^{-1})$ and $\mathcal{M} = O(\epsilon^3)$, and
413 Monophasic, where assumes $\mathcal{V} = O(1)$ and $\mathcal{M} = O(\epsilon^2)$ and additionally assumes the melt
414 network is disconnected. Their derivation is given in the next two sections.

C1. Biphasic-II: Unequal Velocities at the Interface

In this case $\mathcal{V} = O(\epsilon^{-1})$ and $\mathcal{M} = O(\epsilon^3)$. Following the scheme of Section 3.5, the macroscopic equations are

$$\langle \mathbf{v}^{f(0)} \rangle_f = -\frac{\langle K \rangle_f}{\mu_f} (\nabla_x p^{f(0)} - \mathbf{g}^f) \quad (\text{C1})$$

$$\nabla_x \cdot \langle \mathbf{v}^{f(0)} \rangle_f = 0. \quad (\text{C2})$$

415 Multiplying (C1) by V^f and (C2) by V^f/L restores the dimensions of these equations.

C2. Monophasic: Magma Bubbles

As in Biphasic-I, we take $\mathcal{V} = O(1)$ and $\mathcal{M} = O(\epsilon^2)$. However, we now assume that the fluid is not topologically connected. The equations are the same at all orders of ϵ as those appearing in Section 3.5.

Under this assumption on the microscopic geometry, the permeability cell problems, (64a–64c), can be shown to have trivial solutions. $\mathbf{k}^i = 0$ for $i = 1, 2, 3$, so $\langle k \rangle_f = 0$. Because the melt is trapped it must migrate with the matrix,

$$\mathbf{v}^{f(0)}(\mathbf{x}, \mathbf{y}) = \mathbf{v}^{s(0)}(\mathbf{x}) \quad (\text{C3})$$

Combining (C3) with (74), recovers the incompressibility of the matrix,

$$\nabla_x \cdot \mathbf{v}^{s(0)} = 0 \quad (\text{C4})$$

Dropping the divergence terms from (59) completes the system:

$$\begin{aligned} 0 = & \bar{\rho} \mathbf{g} - \nabla_x p^{f(0)} - \nabla_x [2\mu_s e_{x,lm}(\mathbf{v}^{s(0)}) \langle \pi^{lm} \rangle_s] \\ & + 2\mu_s \nabla_x \cdot [(1 - \phi) e_x(\mathbf{v}^{s(0)}) + 2e_{x,lm}(\mathbf{v}^{s(0)}) \langle e_y(\bar{\chi}^{lm}) \rangle_s] \end{aligned} \quad (\text{C5})$$

This is a homogenized incompressible Stokes system for a hybrid material with isolated very low viscosity inclusions.

Appendix D: Non-Homogenizable Regimes

When either $Q_\ell^f \gg \epsilon$ or $Q_\ell^f \ll \epsilon$, the system is non-homogenizable. By this we mean that it is not possible to upscale equations that faithfully preserve our physical assumptions. For instance, if $Q_\ell^f = O(1)$ the pressure gradient balances the viscous forces in the fluid and there is no scale separation. Working out the expansions, the leading order velocity

and pressure in the fluid solve:

$$\nabla_y \cdot [-\tilde{p}^{f(0)} + 2\tilde{\mu}_f e_y(\tilde{\mathbf{v}}^{f(0)})] = 0 \quad \text{in } Y_f \quad (\text{D1})$$

$$\nabla_y \cdot \tilde{\mathbf{v}}^{f(0)} = 0, \quad \text{in } Y_f \quad (\text{D2})$$

$$\tilde{\mathbf{v}}^{f(0)} = 0, \quad \text{on } \gamma \quad (\text{D3})$$

The solution is $\tilde{\mathbf{v}}^{f(0)} = 0$. Therefore,

$$\begin{aligned} \mathbf{v}^{f,\epsilon} &= V^f \tilde{\mathbf{v}}^{f,\epsilon} \\ &= V^f (\tilde{\mathbf{v}}^{f(0)} + \epsilon \tilde{\mathbf{v}}^{f(1)} + \dots) \\ &= \epsilon V^f (\mathbf{v}^{f(1)} + \dots) \end{aligned} \quad (\text{D4})$$

421 This implies that $|\mathbf{v}^{f,\epsilon}| = O(\epsilon V^f)$, contradicting our physical assumption that $|\mathbf{v}^{f,\epsilon}| =$
 422 $O(V^f)$. While this is mathematically reasonable, the model is unable to produce macro-
 423 scopic fluid velocities of order V^f . Other upscaling techniques may succeed here, but
 424 homogenization will not.

Suppose instead $Q_\ell^f = O(\epsilon^2)$ or smaller. The fluid equations are then:

$$O(\epsilon^0) : \quad -\nabla_y \tilde{p}^{f(0)} = 0 \quad \text{in } Y_f \quad (\text{D5})$$

$$O(\epsilon^1) : \quad -\nabla_y \tilde{p}^{f(1)} - \nabla_x \tilde{p}^{f(0)} + \tilde{\mathbf{g}}^f = 0 \quad \text{in } Y_f \quad (\text{D6})$$

The first equation implies $\tilde{p}^{f(0)} = \tilde{p}^{f(0)}(\mathbf{x})$. Since $\nabla_x \tilde{p}^{f(0)}$ and $\tilde{\mathbf{g}}^f$ are independent of \mathbf{y} , $\nabla_y \tilde{p}^{f(1)}$ must also be independent. Since it is periodic in \mathbf{y} , it is zero. But this implies

$$-\nabla_x \tilde{p}^{f(0)} + \tilde{\mathbf{g}}^f = 0 \quad (\text{D7})$$

425 *The leading order macroscopic pressure gradient plays no role in balancing the viscous*
 426 *forces in the solid.* This contradicts our assumption that there is *always* a leading order
 427 non-hydrostatic pressure gradient.

Though our assumption on the non-hydrostatic pressure gradient may seem arbitrary, there is another important reason to identify cases without such a pressure as non-homogenizable. There are problems of interest where gravity plays little role, such as *Spiegelman* [2003]; *Katz et al.* [2006]. In these cases, $\tilde{\mathbf{g}}^f$ would be absent from our equations, including (D7). Hence,

$$\begin{aligned}\nabla p^f &= \frac{P^f}{L} \nabla_x (\tilde{p}^{f(0)} + \epsilon \tilde{p}^{f(1)} + \dots) \\ &= \epsilon \frac{P^f}{L} \nabla_x (\tilde{p}^{f(1)} + \dots) \\ &= O(\epsilon \frac{P^f}{L})\end{aligned}$$

428 This implies the macroscopic fluid pressure gradient is not $O(P^f/L)$, as hypothesized.

Appendix E: Cell Problem Symmetries

429 Let us assume our cell domain is symmetric with respect to the principal axes and
430 invariant under rigid rotations. This permits simplifications of some of the cell problems.

In the Darcy cell problem, the off-diagonal entries become zero while the diagonal entries are all equal. Thus:

$$k_{\text{eff.}} = \langle \mathbf{k}_1^1 \rangle_f \quad (\text{E1})$$

431 For the surface stress problems, when $l \neq m$, $\langle \pi^{lm} \rangle_s = 0$. Only the l, m and m, l entries
432 of the tensor $\langle e_y(\bar{\chi}^{lm}) \rangle_s$ are non-zero. For $l = m$, $\langle \pi^{ll} \rangle_s = \frac{1}{3}(1 - \phi)$ and only the diagonal
433 entries of $\langle e_y(\bar{\chi}^{ll}) \rangle_s$ are non-zero. The trace of all $\langle e_y(\bar{\chi}^{lm}) \rangle_s$ tensors is zero. More can be
434 said about $e_y(\bar{\chi}^{lm})$, but it does not benefit the present analysis. See *Simpson* [2008] or
435 *Simpson et al.* [2008b] for more details.

436 In the dilation stress problem, the off diagonal terms in $\langle e_y(\bar{\xi}) \rangle_s$ vanish, and the diagonal
437 entries are equal to $\frac{1}{3}(1 - \phi)$.

Appendix F: Spatial Variation in Cell Domain and Time Dynamics

If the cells have \mathbf{x} dependence, $Y_f = Y_f(\mathbf{x})$, then it is possible that $\phi = \phi(\mathbf{x})$. This introduces difficulties in (53a), as terms from gradients with respect to the domain now appear. Let us elaborate. For fixed $\mathbf{x} \in \Omega$, we associate a particular cell $Y = Y(\mathbf{x})$, with fluid and solid regions defined by the indicator functions \mathbb{I}_f and \mathbb{I}_s :

$$\mathbb{I}_s : \Omega \times Y \mapsto \{0, 1\} \quad (\text{F1a})$$

$$\mathbb{I}_f : \Omega \times Y \mapsto \{0, 1\} \quad (\text{F1b})$$

Then

$$Y_f(\mathbf{x}) = \{\mathbf{y} \in Y \mid \mathbb{I}_f(\mathbf{x}, \mathbf{y}) = 1\} \quad (\text{F2a})$$

$$Y_s(\mathbf{x}) = \{\mathbf{y} \in Y \mid \mathbb{I}_s(\mathbf{x}, \mathbf{y}) = 1\} \quad (\text{F2b})$$

Returning to (53a),

$$\begin{aligned} & \int_{Y_s} \nabla_x \cdot \sigma^{s(0)} d\mathbf{y} + \int_{Y_f} \nabla_x \cdot \sigma^{f(0)} d\mathbf{y} \\ &= \int_Y \nabla_x \cdot \sigma^{s(0)} \mathbb{I}_s d\mathbf{y} + \int_Y \nabla_x \cdot \sigma^{f(0)} \mathbb{I}_f d\mathbf{y} \\ &= \nabla_x \cdot \int_{Y_s} \sigma^{s(0)} d\mathbf{y} - \int_Y \sigma^{s(0)} \cdot \nabla_x \mathbb{I}_s d\mathbf{y} \\ & \quad + \nabla_x \cdot \int_{Y_f} \sigma^{f(0)} d\mathbf{y} - \int_Y \sigma^{f(0)} \cdot \nabla_x \mathbb{I}_f d\mathbf{y} \end{aligned} \quad (\text{F3})$$

Witness the appearance of the $\nabla \mathbb{I}_s$ and $\nabla \mathbb{I}_f$ terms. *This is only an issue for (53a). The other macroscopic equations remain valid when we allow cell variation.*

A second problem is manifest when we consider time dynamics.

$$\begin{aligned} \partial_t \phi &= \partial_t \int_{Y_f} 1 d\mathbf{y} = \int_{\Gamma} \mathbf{v}^f \cdot \mathbf{n} dS \\ &= - \int_{\Gamma} \mathbf{v}^s \cdot \mathbf{n} dS = - \int_{\Gamma} (\mathbf{v}^{s(0)} + \epsilon \mathbf{v}^{s(1)} + \dots) \cdot \mathbf{n} dS \end{aligned}$$

Since $\mathbf{v}^{s(0)}$ is independent of \mathbf{y} , the first term drops. Substituting (51),

$$\partial_t \phi = -\epsilon \int \nabla_y \cdot \mathbf{v}^{s(1)} d\mathbf{y} + O(\epsilon^2) = \epsilon \nabla_x \cdot \mathbf{v}^{s(0)} (1 - \phi) + O(\epsilon^2)$$

To leading order, the matrix can only vary by dilation and compaction.

Acknowledgments. Both this paper and *Simpson et al.* [2008b] are based on the thesis of G. Simpson, *Simpson* [2008], completed in partial fulfillment of the requirements for the degree of doctor of philosophy at Columbia University.

The authors wish to thank D. Bercovici and R. Kohn for their helpful comments.

This work was funded in part by the US National Science Foundation (NSF) Collaboration in Mathematical Geosciences (CMG), Division of Mathematical Sciences (DMS), Grant DMS-05-30853, the NSF Integrative Graduate Education and Research Traineeship (IGERT) Grant DGE-02-21041, NSF Grants DMS-04-12305 and DMS-07-07850.

References

- Auriault, J., Nonsaturated deformable porous media: Quasistatics, *Transport in Porous Media*, 2(1), 45–64, 1987.
- Auriault, J., Heterogeneous medium. Is an equivalent macroscopic description possible?, *International Journal of Engineering Science*, 29(7), 785–795, 1991a.
- Auriault, J., Poroelastic media, in *Homogenization and Porous Media*, edited by U. Hornung, pp. 163–182, Springer, 1991b.
- Auriault, J., and C. Boutin, Deformable porous media with double porosity. Quasi-statics. I: Coupling effects, *Transport in Porous Media*, 7(1), 63–82, 1992.
- Auriault, J., and P. Royer, Seismic waves in fractured porous media, *Geophysics*, 67, 259, 2002.
- Auriault, J., D. Bouvard, C. Dellis, and M. Lafer, Modelling of Hot Compaction of Metal Powder by Homogenization, *Mechanics of Materials(The Netherlands)*, 13(3), 247–255,

1992.

Bensoussan, A., J. Lions, and G. Papanicolaou, *Asymptotic Analysis for Periodic Structures*, *Studies in Mathematics and its Applications*, vol. 5, Elsevier, 1978.

Bercovici, D., and Y. Ricard, Energetics of a two-phase model of lithospheric damage, shear localization and plate-boundary formation, *Geophysical Journal International*, *152*(3), 581–596, 2003.

Bercovici, D., and Y. Ricard, Tectonic plate generation and two-phase damage: Void growth versus grain size reduction, *Journal of Geophysical Research*, *110*(B3), 2005.

Bercovici, D., Y. Ricard, and G. Schubert, A two-phase model for compaction and damage, 1: General theory, *Journal of Geophysical Research*, *106*(B5), 8887–8906, 2001a.

Bercovici, D., Y. Ricard, and G. Schubert, A Two-Phase Model for Compaction and Damage, 3: Applications to Shear Localization and Plate Boundary Formation, *Journal of Geophysical Research*, *106*, 8925–8939, 2001b.

Brennen, C., *Fundamentals of Multiphase Flow*, Cambridge University Press, 2005.

Chechkin, G., A. Piatnitski, and A. Shamaev, *Homogenization: Methods and Applications*, Translations of Mathematical Monographs, American Mathematical Society, 2007.

Cioranescu, D., and P. Donato, *An Introduction to Homogenization*, Oxford University Press, 1999.

Drew, D., Averaged field equations for two-phase media, *Stud. Appl. Math*, *50*(2), 133–166, 1971.

Drew, D., Mathematical-modeling of 2-phase flow, *Ann. Rev. Fluid Mech*, *15*, 261–291, 1983.

Drew, D., and S. Passman, *Theory of multicomponent fluids*, Springer New York, 1999.

- 484 Drew, D., and L. Segel, Averaged equations for two-phase flows, *Stud. Appl. Math*, 50(3),
485 205–231, 1971.
- 486 Fowler, A., A mathematical model of magma transport in the asthenosphere, *Geophysical*
487 *& Astrophysical Fluid Dynamics*, 33(1), 63–96, 1985.
- 488 Fowler, A., Generation and Creep of Magma in the Earth, *SIAM Journal on Applied*
489 *Mathematics*, 49, 231, 1989.
- 490 Geindreau, C., and J. Auriault, Investigation of the viscoplastic behaviour of alloys in the
491 semi-solid state by homogenization, *Mechanics of Materials*, 31(8), 535–551, 1999.
- 492 Hier-Majumder, S., Y. Ricard, and D. Bercovici, Role of grain boundaries in magma
493 migration and storage, *Earth and Planetary Science Letters*, 248(3-4), 735–749, 2006.
- 494 Hirth, G., and D. Kohlstedt, Experimental constraints on the dynamics of the partially
495 molten upper mantle: Deformation in the diffusion creep regime, *Journal of Geophysical*
496 *Research*, 100(B2), 1981–2001, 1995a.
- 497 Hirth, G., and D. Kohlstedt, Experimental constraints on the dynamics of the partially
498 molten upper mantle 2: Deformation in the dislocation creep regime, *Journal of Geo-*
499 *physical Research*, 100(B2), 15,441–15,449, 1995b.
- 500 Hornung, U., *Homogenization and Porous Media*, Springer, 1997.
- 501 Katz, R., M. Spiegelman, and B. Holtzman, The dynamics of melt and shear localization
502 in partially molten aggregates., *Nature*, 442(7103), 676–9, 2006.
- 503 Katz, R., M. Knepley, B. Smith, M. Spiegelman, and E. Coon, Numerical simulation of
504 geodynamic processes with the Portable Extensible Toolkit for Scientific Computation,
505 *Physics of the Earth and Planetary Interiors*, 163(1-4), 52–68, 2007.

Lee, C., Flow and deformation in poroelastic media with moderate load and weak inertia, *Proceedings of the Royal Society of London. Series A, Mathematical and Physical Sciences*, 460(2047), 2051–2087, 2004.

Lee, C., and C. Mei, Re-examination of the equations of poroelasticity, *International journal of engineering science*, 35(4), 329–352, 1997a.

Lee, C., and C. Mei, Thermal consolidation in porous media by homogenization theory—I. Derivation of macroscale equations, *Advances in Water Resources*, 20(2-3), 127–144, 1997b.

Lee, C., and C. Mei, Thermal consolidation in porous media by homogenization theory—II. Calculation of effective coefficients, *Advances in Water Resources*, 20(2-3), 145–156, 1997c.

McKenzie, D., The generation and compaction of partially molten rock, *Journal of Petrology*, 25(3), 713–765, 1984.

Mei, C., and J. Auriault, Mechanics of Heterogeneous Porous Media With Several Spatial Scales, *Proceedings of the Royal Society of London. Series A, Mathematical and Physical Sciences*, 426(1871), 391–423, 1989.

Mei, C., J. Auriault, and C. Ng, Some applications of the homogenization theory, *Advances in applied mechanics*, 32, 277–348, 1996.

Pavliotis, G., and A. Stuart, *Multiscale Methods: Averaging and Homogenization*, Springer, 2008.

Peter, M., Homogenisation of a chemical degradation mechanism inducing an evolving microstructure, *Comptes rendus-Mécanique*, 335(11), 679–684, 2007a.

- 528 Peter, M., Homogenisation in domains with evolving microstructure, *Comptes rendus-*
529 *Mécanique*, 335(7), 357–362, 2007b.
- 530 Peter, M., Coupled reaction–diffusion processes inducing an evolution of the microstruc-
531 ture: Analysis and homogenization, *Nonlinear Analysis*, 70, 806–821, 2009.
- 532 Ricard, Y., Physics of mantle convection, in *Treatise on Geophysics*, vol. 7, edited by
533 G. Schubert, Elsevier, 2007.
- 534 Ricard, Y., and D. Bercovici, Two-phase damage theory and crustal rock failure: the
535 theoretical ‘void’ limit, and the prediction of experimental data, *Geophysical Journal*
536 *International*, 155(3), 1057–1064, 2003.
- 537 Ricard, Y., D. Bercovici, and G. Schubert, A two-phase model of compaction and damage,
538 2: Applications to compaction, deformation, and the role of interfacial surface tension,
539 *Journal of Geophysical Research*, 106, 8907–8924, 2001.
- 540 Sanchez-Palencia, E., *Non-homogeneous media and vibration theory*, Lecture Notes in
541 Physics, 127, 1980.
- 542 Schmeling, H., Partial melting and melt segregation in a convecting mantle, in *Physics*
543 *and Chemistry of Partially Molten Rocks*, edited by N. Bagdassarov, D. Laporte, and
544 A. Thompson, pp. 141–178, Kluwer Academic, 2000.
- 545 Scott, D., and D. Stevenson, Magma solitons, *Geophysical Research Letters*, 11(11), 1161–
546 1161, 1984.
- 547 Scott, D., and D. Stevenson, Magma ascent by porous flow, *Journal of Geophysical Re-*
548 *search*, 91, 9283–9296, 1986.
- 549 Simpson, G., The mathematics of magma migration, Ph.D. thesis, Columbia University,
550 2008.

Simpson, G., M. Spiegelman, and M. Weinstein, A multiscale model of partial melts 1:

Effective equations, submitted to Journal of Geophysical Research, 2008a.

Simpson, G., M. Spiegelman, and M. Weinstein, A multiscale model of partial melts 2:

Numerical results, submitted to Journal of Geophysical Research, 2008b.

Spiegelman, M., Flow in deformable porous media. part 1: Simple analysis, *Journal of*

Fluid Mechanics, 247, 17–38, 1993.

Spiegelman, M., Linear analysis of melt band formation by simple shear, *Geochemistry,*

Geophysics, Geosystems, 4(9), 8615, 2003.

Spiegelman, M., R. Katz, and G. Simpson, An Introduction and Tutorial to the

“McKenize Equations” for magma migration, [http://www.geodynamics.org/cig/](http://www.geodynamics.org/cig/workinggroups/magma/workarea/benchmark/McKenzieIntroBenchmarks.pdf)

[workinggroups/magma/workarea/benchmark/McKenzieIntroBenchmarks.pdf](http://www.geodynamics.org/cig/workinggroups/magma/workarea/benchmark/McKenzieIntroBenchmarks.pdf), 2007.

Stevenson, D., and D. Scott, Mechanics of Fluid-Rock Systems, *Annual Review of Fluid*

Mechanics, 23(1), 305–339, 1991.

Temam, R., *Navier-Stokes Equations: Theory and Numerical Analysis*, American Math-

ematical Society, 2001.

Torquato, S., *Random Heterogeneous Materials: Microstructure and Macroscopic Proper-*

ties, Springer, 2002.

Wark, D., and E. Watson, Grain-scale permeabilities of texturally equilibrated, monomin-

eralic rocks, *Earth and Planetary Science Letters*, 164(3-4), 591–605, 1998.

Table 1. Notation for domains in homogenization model.

Symbol	Meaning
γ	Interface between melt and matrix within cell Y
Γ	Total macroscopic interface between melt and matrix
Ω	Total macroscopic space occupied by both melt and matrix
Ω_f	Portion of macroscopic space occupied by melt
Ω_s	Portion macroscopic space occupied by matrix
Y	The unit cell
Y_f	Portion of unit cell occupied by melt
Y_s	Portion of unit cell occupied by matrix

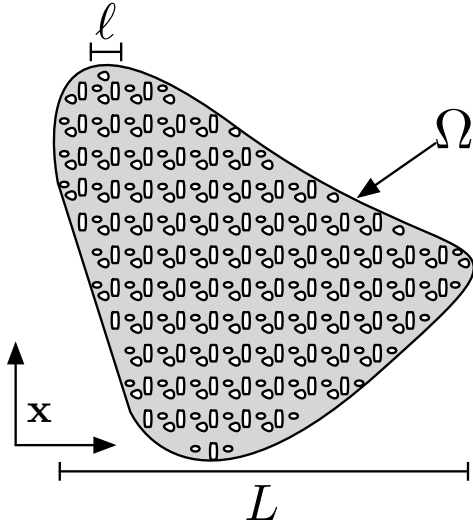


Figure 1. The macroscopic domain Ω . The matrix occupies the gray region while the melt occupies the white inclusions.

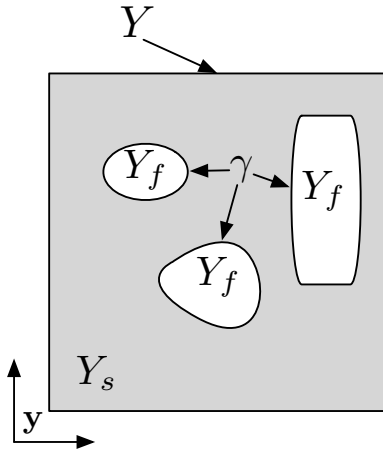


Figure 2. The cell domain, Y , divided into fluid and solid regions, Y_f and Y_s . The two phases meet on interface Γ .

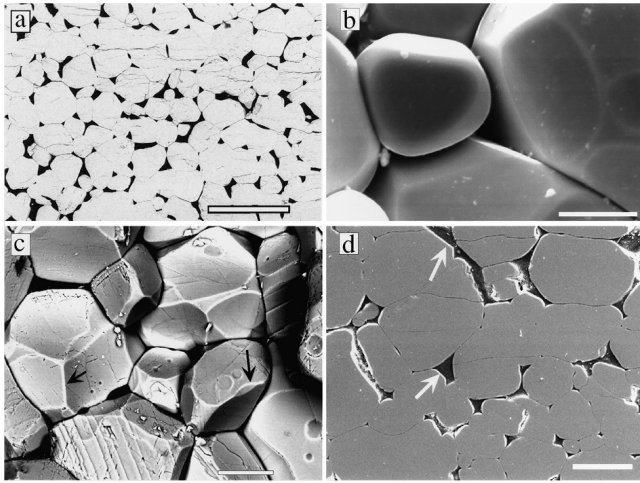


Figure 3. SEM images of synthetic quartzites and marbles from Figure 5 of *Wark and Watson* [1998]. Similar microstructures are seen in olivine basalt aggregates [e.g. *Hirth and Kohlstedt*, 1995a, b]

Table 2. Notation for fields in homogenization model.

Symbol	Meaning
$e(\mathbf{v})$	Strain rate tensor, $e(\mathbf{v}) = \frac{1}{2}(\nabla \mathbf{v} + (\nabla \mathbf{v})^T)$
ϕ	Volume fraction of melt, $\phi \equiv \int_{Y_f} d\mathbf{y}$
\mathbf{g}	$-g\mathbf{z}$
\mathbf{g}^f	$\rho_f \mathbf{g}$
\mathbf{g}^s	$\rho_s \mathbf{g}$
p^f	Melt pressure
$p^{f(j)}$	Melt pressure at order j in the series expansion
p^s	Melt pressure
$p^{s(j)}$	Matrix pressure at order j in the series expansion
σ^f	Melt Stress Tensor
$\sigma^{f(j)}$	Melt Stress Tensor at order j in the series expansion
σ^s	Matrix Stress Tensor
$\sigma^{s(j)}$	Matrix Stress Tensor at order j in the series expansion
\mathbf{v}^f	Melt velocity
$\mathbf{v}^{f(j)}$	Melt velocity at order j in the series expansion
\mathbf{v}^s	Matrix Velocity
$\mathbf{v}^{s(j)}$	Matrix velocity at order j in the series expansion

Table 3. Notation and measurements for models of partial melts.

Symbol	Meaning	Value
ϕ	Volume Fraction of Melt	.01%– 10%
g	Gravity	9.8 m/s ²
ℓ	Grain Length Scale	1 –10 mm
L	Macroscopic Length Scale	1 m - 10 km
μ_f	Melt Shear Viscosity	1–10 Pa s
μ_s	Matrix Shear Viscosity	10 ¹⁵ –10 ²¹ Pa s
Re_ℓ^f	Reynolds Number of Melt	10 ⁻⁸ –10 ⁻⁵
Re_ℓ^s	Reynolds Number of Matrix	10 ⁻³⁰ –10 ⁻²²
ρ_f	Melt Density	2800 kg/m ³
ρ_s	Matrix Density	3300 kg/m ³
V^f	Characteristic Melt Velocity	1 – 10 m/yr
V^s	Characteristic Matrix Velocity	1 – 10 cm/yr

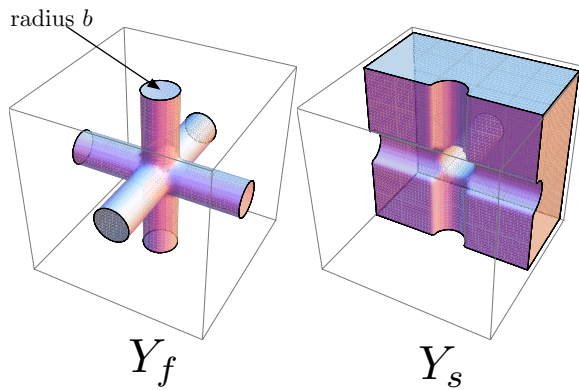
**Figure 4.** A cell geometry in which both the fluid region, Y_f , and the solid region, Y_s , are topologically connected.

Table 4. Dimensionless numbers for homogenization model.

Symbol	Meaning	Estimate
ϵ	Length scale ratio, $\epsilon = \ell/L$	$O(10^{-7} - 10^{-2})$
\mathcal{M}	Viscosity ratio, $\mathcal{M} = \mu_f/\mu_s$	$O(10^{-21} - 10^{-14})$
\mathcal{P}	Pressure ratio, $\mathcal{P} = P^f/P^s$	$O(\epsilon^0)$
\mathcal{Q}_ℓ^f	Ratio of viscous force to pressure gradient in melt, $\mathcal{Q}_\ell^f = (\mu_f V^f)/(P^f \ell)$	$O(\epsilon^9 - \epsilon^0)$
\mathcal{Q}_ℓ^s	Ratio of viscous force to pressure gradient in matrix, $\mathcal{Q}_\ell^s = (\mu_s V^s)/(P^s \ell)$	$O(\epsilon^{-1})$
\mathcal{Q}_L^s	Ratio of viscous force to pressure gradient in matrix, $\mathcal{Q}_L^s = (\mu_s V^s)/(P^s L)$	$O(\epsilon^0)$
\mathcal{R}_ℓ^f	Ratio of buoyancy force to pressure gradient in melt, $\mathcal{R}_\ell^f = (\rho_f g \ell)/P^f$	$O(\epsilon^1)$
\mathcal{R}_ℓ^s	Ratio of buoyancy force to pressure gradient in matrix, $\mathcal{R}_\ell^s = (\rho_s g \ell)/P^s$	$O(\epsilon^1)$
\mathcal{R}_L^s	Buoyancy force to pressure gradient ratio in matrix, $\mathcal{R}_L^s = (\rho_s g L)/P^s$	$O(\epsilon^0)$
\mathcal{V}	Velocity ratio, $\mathcal{V} = V^f/V^s$	$O(10^{-7} - 10^{-2})$

Table 5. Effective quantities derived by homogenization.

Symbol	Meaning
η_{eff}	Effective supplementary anisotropic viscosity, a fourth order tensor. $\eta_{\text{eff}}^{lm} = 2\mu_s \langle \bar{\chi}^{lm} \rangle_s$ is a second order tensor.
$\langle K \rangle_f$	Permeability, a second order tensor. The i-th column is given by $\langle \mathbf{k}^i \rangle_f$.
k_{eff}	Isotropic permeability. Under symmetry, $k_{\text{eff}} = \langle \mathbf{k}_1^1 \rangle_f$
$\langle \cdot \rangle_f$	Volume average of a quantity over the melt portion of a cell, $\langle \cdot \rangle_f = \int_{Y_f} \cdot d\mathbf{y}$
$\langle \cdot \rangle_s$	Volume average of a quantity over the matrix portion of a cell, $\langle \cdot \rangle_s = \int_{Y_s} \cdot d\mathbf{y}$
P	Effective macroscopic (fluid) pressure, $P = p^{f(0)}$.
\mathbf{V}^f	Effective macroscopic fluid velocity, $\mathbf{V}^f = \langle \mathbf{v}^{f(0)} \rangle_f / \phi$.
\mathbf{V}^s	Effective macroscopic solid velocity, $\mathbf{V}^s = \mathbf{v}^{s(0)}$.
ζ_{eff}	Effective bulk viscosity of the matrix, $\zeta_{\text{eff}} = \mu_s \langle \zeta \rangle_s - \frac{2}{3}\mu_s(1 - \phi)$

Table 6. Notation for cell problems.

Symbol	Meaning
$\bar{\chi}^{lm}$	Velocity of the cell problem for a unit shear stress forcing on the solid in the lm component of the stress tensor
\mathbf{e}_i	Unit vector in the i -th coordinate, $\mathbf{e}_1^T = (1, 0, 0)$
\mathbf{k}^i	Velocity of the cell problem for a unit forcing on the fluid in the \mathbf{e}_i direction
$\bar{\xi}$	Velocity of the cell problem for a unit forcing on the divergence equation
π^{lm}	Pressure of the cell problem for a unit shear stress forcing on the solid in the lm component of the the stress tensor
q_i	Pressure of the cell problem for a unit forcing on the fluid in the \mathbf{e}_i direction
ζ	Pressure of the cell problem for a unit forcing on the divergence equation

Table 7. Additional notation for the other models.

Symbol	Meaning
C_0	An $O(1)$ Constant
κ	Permeability
κ_0	Permeability constant for a power law permeability, $\kappa = \kappa_0 \phi^n$
ζ_s	Bulk viscosity